University of Southern Queensland

Faculty of Health, Engineering, and Sciences

Investigation into the Influence of Double Bagging Processes on Co-cured Scarf Repairs

A dissertation submitted by

Riley Malcolm Mitchell

In fulfilment of the requirements of

ENG4111 and ENG4112 Research Project

Towards the degree of

Bahcelor of Engineering (Honours)- Mechanical

Submitted October 2019

Abstract

The prevalence of non-monolithic materials such as carbon fibre reinforced polymers (CFRP) in aerospace has introduced many new complexities to the materials industry. Sustainment and through life costs of military vehicles are often substantially greater than acquisition costs, and as such, efforts to improve reliability and minimise costs are significant. Regarding composite structures, scarf repairs are often used to restore strength to a damaged component, with a shifting focus to out-of-autoclave processes to reduce cost. The aim of this project was to identify the effects of processing techniques through the application of novel and standard assessment techniques.

Through the application of novel techniques, including pressure mapping and cure kinetics modelling, relationships surrounding bond quality and quality control were established. It was observed throughout this project that comparable strength and quality for DVB co-cured specimens with improved quality control was achieved when a caul plate was utilised. With consistent cohesive substrate failure (CSF) observed, 0.03 +/- 0.038 % average bond-line porosity, and an average tensile strength of 401 +/- 28 MPa, the quality and consistency of these specimens was significantly greater than other co-cured groups. It was also observed that the DVB cure cycle, when applied to the hard patch approach, resulted in decreased average tensile strength, indicative of an improper cure cycle. Cure kinetics modelling applied to the adhesive saw that the DVB process delayed the onset point by approximately 5°C and 30 minutes.

Additional work is required surrounding the cure kinetics for the prepreg system, in order to establish an optimized theoretical cure process. Additionally, further mechanical testing, porosity evaluation, and dielectric cure sensing will offer additional insights into the DVB co-curing process, allowing for standardized repair procedures to be developed.

Limitations of Use

University of Southern Queensland

Faculty of Health, Engineering and Sciences

ENG4111/ENG4112 Research Project

The Council of the University of Southern Queensland, its Faculty of Health, Engineering & Sciences, and the staff of the University of Southern Queensland, do not accept any responsibility for the truth, accuracy or completeness of material contained within or associated with this dissertation.

Persons using all or any part of this material do so at their own risk, and not at the risk of the Council of the University of Southern Queensland, its Faculty of Health, Engineering & Sciences or the staff of the University of Southern Queensland.

This dissertation reports an educational exercise and has no purpose or validity beyond this exercise. The sole purpose of the course pair entitled "Research Project" is to contribute to the overall education within the student's chosen degree program. This document, the associated hardware, software, drawings, and other material set out in the associated appendices should not be used for any other purpose: if they are so used, it is entirely at the risk of the user

Certification of Dissertation

University of Southern Queensland

Faculty of Health, Engineering and Sciences

ENG4111/ENG4112 Research Project

I certify that the ideas, designs and experimental work, results, analyses and conclusions set out in this dissertation are entirely my own effort, except where otherwise indicated and acknowledged.

 I further certify that the work is original and has not been previously submitted for assessment in any other course or institution, except where specifically stated.

Riley Mitchell

Signature

16/10/2019

Acknowledgements

Table of Contents

List of Figures

List of Tables

1. Introduction

1.1 Chapter Overview

This chapter will offer an insight to the current materials and aerospace landscape and establish the foundation of how this project intends to influence the repair of composite aircraft. The development of research aims will provide an insight into the direction of this project, with the contextual information provided within the research background.

1.2 Research Background

As non-monolithic materials such as Carbon Fibre Reinforced Polymers (CFRPs) become more prevalent in the materials sector, implications on the aerospace industry cannot be overstated. With an extremely vast array of applications in aerospace, Mauritz (2012, p.1) defines these materials as "structural materials intended to carry flight induced loads". This, by definition, includes significant structural components such as wings and fuselages, to more intricate objects such as structural jet engine components.

Due to the "never-ending demands for high performance aerospace vehicles with lightweight, highly reliable and durable structures" (Prasad & Wanhill 2017), it is paramount that the materials industry be able to provide novel solutions and sound analytical assessment of this technology. With demands such as sustained supersonic flight, high cruise altitudes, and extreme maneuverability, potential material solutions are continually exposed to more harsh conditions and flight loads. Due to these high-performance rigorous, in conjunction with the need to reduce financial output and supply wait times, according to Soutis (2005), Fibre Reinforced Polymers (FRPs) such as CFRPs, will continue to replace conventional aerospace materials such as aluminium alloys (Al-alloys) and titanium alloys (Ti-alloys).

Unlike typical monolithic materials such as Al and Ti alloys, the mechanical properties of FRPs are tailorable given fibre orientation and chosen fibre/resin systems, lending to the concept that they have advanced manufacturability and conformability. With desirable properties such as high strength-to-weight ratios, corrosion resistance, and ability to produce more complex shapes (Bhagwat et al. 2016), this also leads to suggest that FRPs will, according to Holmes (2017), help absorb the current 10-year backlog currently being experienced by aircraft manufacturers.

However, as desirable as FRPs appear, they also experience more complex shortcomings compared to traditional materials. FRPs shortcomings, more precisely CFRPs for this project, are generally related to the behaviour and interaction of the epoxy polymer and carbon fibre matrix (Mouritz 2012) and manufacturing method. The anisotropic nature of the fibres, along with the need for skilled production means that failure behaviour is somewhat harder to understand. These shortcomings, which were formerly addressed for autoclave manufacturing processes, are now being re-experienced with the current industry demand for Out-of-Autoclave (OOA) repair systems for aircraft. This OOA repair technology, and, more precisely, the reduction of void content and applications of advanced sensing technology, is this foundation of this project, and will be further explored in the proceeding literature review.

1.3 Project Aim

The aim of this paper was to assess the influence of the double vacuum bag method on scarfed aircraft repairs, using out-of-autoclave processing techniques. The scope of this project is limited to assessing the quality of a co-cured (soft patch and adhesive) scarf repair compared to a hard patch approach, and whether the quality of this co-cured specimen is comparable regarding porosity content and strength.

1.4 Project Objectives

To assess the aforementioned aim, this dissertation will follow a set of objectives outlined below. These are closely likened to that supplied in Appendix A, to ensure transparency within this study.

   I.   Identify and deconstruct the processing materials and techniques to ensure a strong knowledge foundation is established and correct processing techniques are followed.

   II.   Identify the underlying defect and unique repair related concepts, to allow for relationships to be developed between said concepts and processing techniques.

   III. Analyse previous appropriate studies to assess experimental and overall methodologies, to ensure appropriate machining techniques and mechanical and material property assessments are conducted.

   IV.   Produce parent specimens using identified processing techniques, followed by appropriate surface machining and preparation, scarf layup and co-cure.

V.   Conduct predetermined mechanical and material assessments, determining relationships between results, processing techniques, and defect concepts.

VI.   Draw final conclusions from the study, making suggestions regarding validity and potential application of OOA processing as a viable and more economical alternative to standard autoclave scarf repairs.

1.5 Chapter Summary

As has been highlighted, the area of OOA processing of composites is an area of significant growth with significant potential for application within the aerospace industry. However, due to the new nature of such systems, processing defects and mechanical behaviour are not well understood, and further study is required to make OOA a viable and effective option for reducing processing time and costs. This paper will address the double vacuum bagging process and its effects on carbon fibre scarf repairs, as required by DSTG. This is intended to determine whether the quality and mechanical performance of such repairs is comparable to the current industry standard of autoclave cured repairs, and the implications of this for reduced aircraft downtime, lower overheads, and less logistics.

2 Literature Review

2.1 Chapter Overview

The intent of this chapter is to identify and analyse the constraining variables, current processing technology, and observe knowledge gaps within current studies. This will firstly be achieved by deconstructing the prepreg system and OOA processing techniques, which are the foundation of this study, preceded by the introduction of defect mechanisms, scarf repair technique, and the assessment methods required for mechanical and microstructure analysis.

2.2 Carbon Fibre Pre-Impregnated (Prepreg) System

Aforementioned, CFRPs are an epoxy resin and carbon fibre matrix system, where the epoxy polymer provides ductility whilst the carbon fibre matrix introduces rigidity, stiffness, and strength (Mouritz 2012). According to ASM Handbooks Online (2001), CFRPs are seven times stronger, two times stiffer, and 1.5 times lighter when compared to 6061 Al-alloy. CFRPs also display fatigue properties superior to any known metal, as well as superior corrosion resistance, lending to their ever-growing applications in aerospace. These polymers, when employed in the aerospace sector, are more commonly referred to as "advanced composites", which are defined by Kutz (2002, p.1132) as "materials consisting of high-stiffness continuous-fibre within a comparatively weak matrix."

To counteract the anisotropic behaviour of unidirectional (UD) fibre reinforcements, and for application in a prepreg system, the desired properties are achieved by layering and consolidating thin lamina at different orientations with an polymer matrix. A pre-impregnated system, known as a prepreg, is a two-part sheet consisting of a partially cured resin (epoxy for this study), and a fibre lamina (the above stated carbon fibre lamina) (Mouritz 2012). The process involves saturating the lamina in a 40-50% solid resin solution, then pressing these lamina sheets together to form prepreg sheets, which is in a partially cured, semi-solid state. This partially cured state is known as B-stage cure, and displays polymer chain crosslinking between about 15-30%, with a fibre content of 58-64%. For use within aerospace applications, these prepreg sheets are generally laid with a [0/+45/-45/90] pattern, depicted in the below figure. This configuration produces quasi-isotropic behaviour, where the properties are all roughly equal when loaded in in-plane directions.
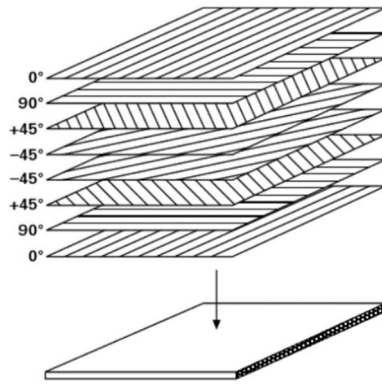
Figure 2-1: [0/+45/-45/90] prepreg layering pattern (Mouritz 2012, p.322).

The appeal of partially impregnated fibre tows was first observed in the 1980's, where, according to Centea et al. (2017), a fully impregnated laminate experienced significant porosity, while the partially impregnated tows displayed almost void-free properties. Another significant characterization of Vacuum-Bag-Only (VBO) prepreg systems, is the presence of engineered vacuum channels (EVaCs). This permeable network of unimpregnated fibres described Centea et al. (2017), allow for gas transportation to occur in-plane, which assists in void reduction and the removal of volatiles within the system.

2.3 Cure Cycle and Double Vacuum Debulking

As previously stated, the composite prepregs exist in what is known as B-stage cure, before final curing in an autoclave, or with an SVD or DVD system. Referring to Loos & Springer (1983), the curing is achieved by consolidating the plies under high pressures to ensure void formation is counteracted, while the elevated temperatures initiate and maintain chemical reactions. Significant variation in curing process between autoclave and OOA is observed with initial and post-cure, with an initial cure for an OOA system, according to Centea et al. (2014), of 80-120°C, and a vacuum-held or free-standing post-cures held at up to 177°C. These conditions, predetermined by manufacturer, are optimized to ensure void formation is limited, and maximum desired strengths are achieved, and will be unique for each material and manufacturing system.

An area of interest for this project is surrounding DVB soft patch curing. This method, known as in-situ co-cured soft patch configuration, sees the scarf prepreg and bond cured in a single process. These in-situ processes, when conducted using SVD systems, were limited by the ability to apply uniform elevated temperatures and high pressures. Centea & Hubert (2011) acknowledge that the maximum

achievable pressure using an SVD system is 1atm, and that due to the load also shared by the fibre bed, the pressure is often not enough to evacuate all volatiles and consolidate the fibres fully, resulting in a material of high porosity. These observed deformities such as high porosity levels, which according to Feng et al. (2019), for each 1% increase in porosity levels between 0 and 4%, a 9% strength decrease for interlaminar shear is experienced, meant a more appropriate curing system was required.

The proposed DVD system, developed in the 1980's, produces debulking at vacuum conditions without the presence of compaction, achieved by applying a second vacuum via a rigid structure (Chong et al. 2018). The configuration utilised for this method is depicted below in Figure 5.
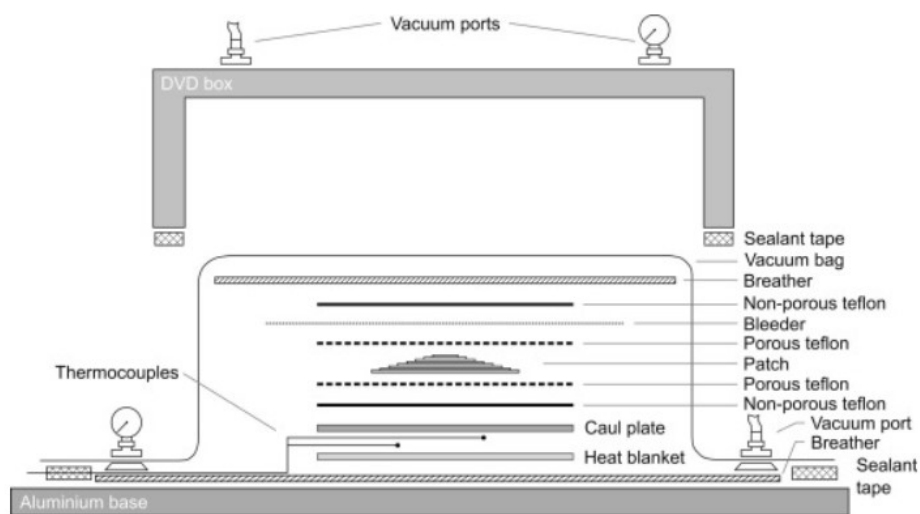
Figure 2-2: DVB configuration (Chong et al. 2018).

Unlike SVD where compaction forces are present due to the pressure application being applied directly to the caul, this is eliminated using a DVB process while still maintaining the vacuum effectiveness, as stated by Hou & Jensen (2004). This is achieved by applying the outer vacuum over a rigid box intermediate the two vacuum environments, which elements compaction pressure during the initial ramp and hold stages when both vacuums are applied. The outer vacuum is released after the initial ramp and hold, with the final cure occurring under SVB conditions, where the compaction pressure is present, which helps consolidate the laminate.

As observed in the figure, there are a vast arrange of components required in this system, none more so important than the bleeder and breather. These two components allow for the evacuation of volatiles and air through the EVaCs when the consolidation pressure is applied, which produces a part with lower porosity (Centea et al. 2017). Unlike autoclave manufacture where this is not required due to the high external pressures produced, the low consolidation pressures and lower temperatures

produced through DVD manufacturing require these additional components to produce autoclave quality parts.

The method involves using a low initial temperature ramp-and-hold period, with a higher vacuum applied to than outer bag than that of the inner bag. As observed by Hou & Jensen (2004), this operation removes the compaction on the prepreg patch, allowing for volatiles to be evacuated through the inner bag vacuum. At the end of this B-stage cure, the outer bag vacuum is removed whilst the inner vacuum is increased, consolidating the prepreg by compaction through the caul plate, under a high temperature ramp-and-hold Stage 2 cure. Optical micrography comparisons between SVB and DVB debulking, as conducted by Hou & Jensen (2004), are depicted below in Figure 7.
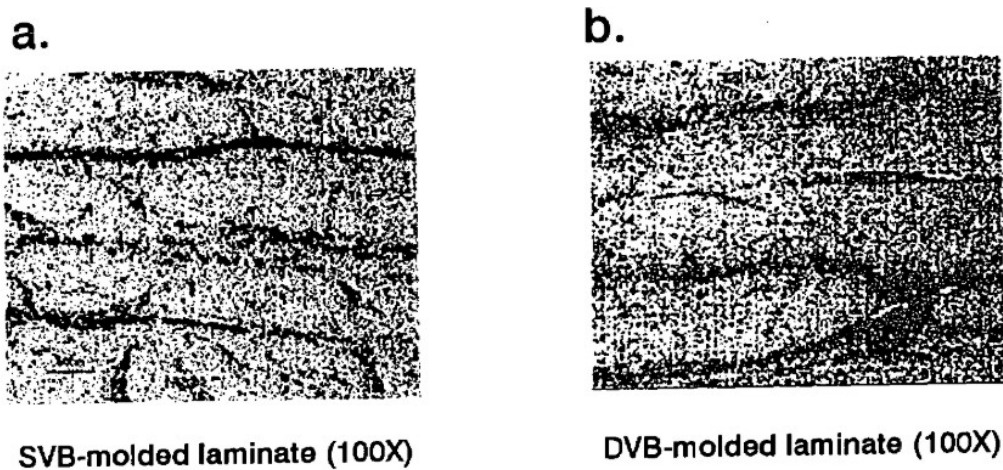
Figure 2-3: Optical micrographic images produced by Hou and Jensen (2004).

As observed in Figure 6, the void formation is significantly reduced using a DVD system. This supports the statements made by Hou & Jensen (2004) that evacuation of volatiles is improved with the DVB method compared to the SVB method, and that this produces a high-quality laminate with lower void formation.

Chong et al. (2018) conducted various experimental comparisons between autoclave, DVD, and hotbonding curing processes to determine void content and specimen strength. The results of the study are summarised in the below table:

Process		Porosity (%)	Tensile modulus (GPa)	Tensile strength (MPa)	Flexural modulus (GPa)	Flexural strength (MPa)	Interlaminar shear strength (MPa)
Patch only	Hotbonding	0.5 ± 0.1	44 ± 2	580 ± 47	34 ± 1	681 ± 27	65 ± 3
	DVD	0.2 ± 0.1	45 ± 2	615 ± 39	37 ± 1	745 ± 10	63 ± 2
	Autoclave	0.0 ± 0.0	45 ± 1	658 ± 19	40 ± 2	746 ± 29	67 ± 2

As expected, the parts produced in an autoclave produced the highest quality for all assessed variables and displayed the expected 0% porosity. The hotbonding manufactured part, defined by Chong et al. (2018) as a DVD cured specimen without the use of DVD preparation such as pre-cure, produced significantly worse properties, most notably the high porosity. However, the quality of the parts produced using the DVD method produced a part with qualities within 90% of the autoclave specimen, even without an adapted OOA cure cycle.

2.4 Porosity and Defects

The most significant issues that arise with composite production, as identified by Baker (1986), are porosity, resin rich and dry areas, insufficient consolidation, and uneven cure. The formation of voids within the composite laminate, which lend themselves to porosity, are critical imperfection, and their presence results in a weakened component. To fully understand voids, it's important to understand the characteristics of both bulk porosity and resin voids, their growth, and how to limit their affects. The below image depicts the various forms of porosity present in a prepreg layup.
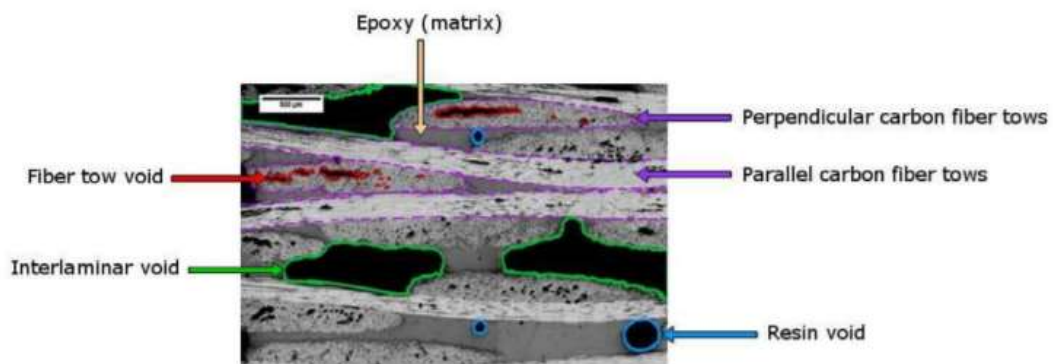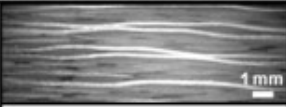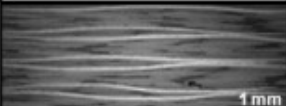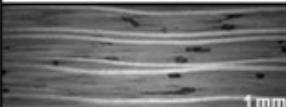
Figure 2-4: Microstructure of a prepreg layup depicting various voids present (Fahrang et al. 2016).

To successfully eliminate the presence of voids in a laminate, Fernlund et al. (2015) states that gases must be fully removed from the voids, which must be then fully infiltrated with resin early in the cure process, while the viscosity of the resin is high, whilst simultaneously limiting the growth of resin voids caused by moisture and volatiles. The steps outlined by Fernlund et al. (2015) and Fahrang et al. (2016) to achieve this are:

- Air must be evacuated by the application of a vacuum, allow adequate time for all gases to be removed, while maintaining high resin viscosity to ensure EVaCs remain open;
- Resin pressure must exceed vapour pressure at all times throughout the cure, to suppress the growth of volatiles through vaporisation; and,
- Resin fills the evacuated voids, which requires low resin viscosity, low void pressure, and high resin pressure.

The slow temperature ramp rate used during the initial stages of the cure, which is applied under vacuum, allow for the evacuation of entrapped gases in fibre tow voids and interlaminar voids. However, supressing the growth of resin voids is more difficult due to the hygroscopic nature of epoxy (Fernlund et al. 2016), which can result in a 1% weight growth due to water absorption. A study conducted by Grunenfelder & Nutt (2010) focused on the effect of void content based on moisture diffusion by exposure in a controlled humidity environment. The results of their study, depicted below, show that exposure to increasing humidity has a significant effect on the porosity exhibited in the final laminate.

Table 2-2: Effect of moisture absorption on void growth (Grunenfelder & Nutt 2010)

VBO Laminates		Void Content (Vol %)	Thickness (mm)
As Received		<<.1	5.08 ± .01
70% RH		.08 ± .08	5.13 ± .01
80% RH		1.00 ± .29	5.31 ± .05
90% RH		2.62 ± .48	5.48 ± .02

However, their results also showed that moisture absorption didn't create any voids, and also had minimal effect on thickness, when the prepreg was autoclave cured. This agrees with the statements from Fernlund et al. (2015) and Fahrang et al. (2016) that resin pressure must exceed vapour pressure to supress resin void growth due to vaporisation. Whereas an autoclave can apply upwards of 6atm pressure, the SVD method can only apply a maximum of 1atm pressure, which is not all applied to the resin, and therefore voids cannot be supressed. There is a gap in knowledge currently on the effect of moisture absorption on void growth in DVD manufacturing, which has the possibility to be investigated within this study.

2.5 Bonded Scarf Repair

The repair of damaged composites is an intricate operation but can provide significant cost reduction benefits when compared to replacing the damaged component whilst restoring strength up to 80% of the undamaged laminate (Caminero et al. 2013). Bonded scarf repair, which will be the focus of this study, displays the highest joint efficiency of any repair method (Caminero et al. 2013), and is the most appropriate where aerodynamic performance is paramount, or a thick specimen must be repaired. Various forms of scarf repairs can be conducted, such as a hard mould repair, but a soft-patch approach, which sees a non-cured prepreg patch laid up with the adhesive in the removal area, then cured in one process, will be used for this study. A significant factor when laying up a scarf repair is that the repair prepreg must be laid in the same pattern and orientation as the parent material, to ensure mechanical loads are distributed uniformly. The below image, courtesy of Gunnion & Wang (2009), depicts the typical 3D scarf repair method, where a uniform tapered, circular scarf is removed.
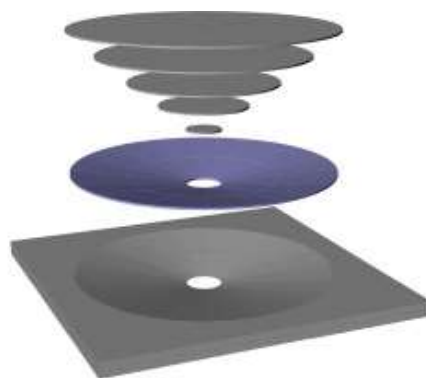
Figure 2-5: Typical 3D scarf repair, depicting scarf removal area, adhesive bond (blue circle), and ply layup (Gunnion & Wang 2009).

The above diagram depicts a repair which is suitable for a quasi-isotropic specimen, but, referring to Gunnion & Wang (2009), can be viewed as overly conservative. The machining of this scarf design, and preparation of the repair plies is quite difficult, and may not be the most suitable option to undertake, as more parent specimens will be required, and will offer less tests per panel.

Another form of scarf repair, often used for simplified testing, is known as a 2D Scarf. The 2D repair method has been extensively studied by Li et al. (2016) and Chong et al. (2018) and offers a more simplistic approach to testing than the abovementioned 3D repair. A 2D repair method takes a tabular form, as depicted in the below image, which is suitable for various mechanical test.

Figure 2-6: Representative top view (left) and side view (right) (Chong et al. 2018).

This simplified repair will allow for less parent material to be produced for a larger quantity of test specimens, while still producing valid results. Chong et al. (2018) make reference to previous studies, which are supported by their results, that a 2D repair will display strength of 50-70% of the parent specimen, providing a baseline for expected results. This design can be simplified further to a scarf specimen, where only one scarf is observed. This design will be the most effective to assess the desired parameters (as identified in the Methodology), as it limits the variables which may fail.

2.6 Scarf Repair Behaviour

When conducting a scarf repair, it is imperative to understand the behaviour of the stress distribution and maximum allowable stress, which is dependent on scarf angle and adhesive strength. The maximum experienced adhesive shear stress, experienced in the circular scarf repair is given by Gunnion & Wang (2009) in equation 1 as:

$$\tau_{max} = \frac{\sigma_{applied}}{2} sin2\alpha \qquad\qquad 1$$

Given the maximum applicable adhesive shear stress, an appropriate scarf angle based upon the maximum shear stress is found to be:

$$\alpha = \frac{1}{2} sin^{-1}(\frac{2\tau_{average}}{\sigma_{xx}}) \qquad\qquad 2$$

This approach can be applied to the study, if a circular scarf is utilised, to ensure a suitable/optimal angle for repair specimens, which will remain consistent, can be utilized. It can be seen in the below

12

figure that the stress distribution for a circular scarf repair displays significantly lower stress in the out-of-plane direction but displayed the lowest maximum shear of the three repair geometries assessed by Gunnion & Wang (2009).
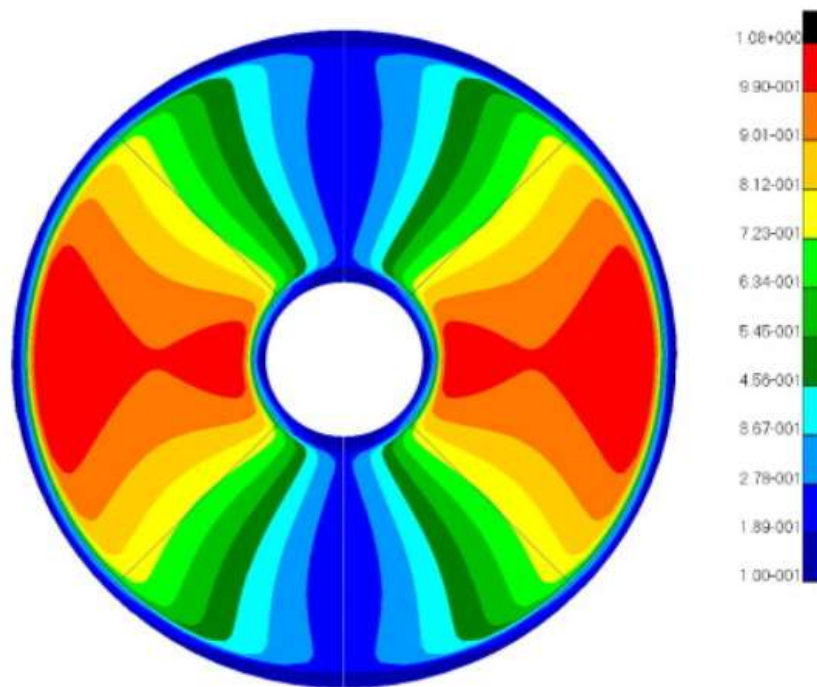
Figure 2-7: Stress distribution behaviour of a circular scarf repair (Gunnion & Wang 2009).

It is also noted in the above figure that the distribution is uniform about both the x and y axis, suggesting that the behaviour be predictable, as well as that the most significant stresses occuring around the internal bond-line, where abrupt geometry and fibre termination occur. The application of the scarf repair technique is further justified by the Caminero et al. (2013) study, where it was assessed and compared against the more simplistic external bonded patch repair technique, showing superior results. However, both Gunnion & Wang (2009) and Caminero et al. (2013) make note of the complexity of conducting a successful scarf repair.

2.7 Bond-line Stress Behaviour

The parametric study conducted by Gunnion & Herzberg (2006), analyses the behaviour of 2D scarf repair under varying conditions. Of major importance, is their analysis of stress behaviour along the

bond line with varying laminate thickness and orientation, scarf angle, and mismatched plies. The below table summarizes the results of their study:

Table 2-3: Results of the Gunnion & Herzberg (2006) study.

Parameter	Average peel	Peak peel	Average shear	Peak shear
Stacking sequence	No effect	Increases if 0° plies are on the outer surfaces	No effect	Decreases with more 0° plies Increases with increasing distance between 0° plies across the scarf
Laminate thickness	No effect	Decreases with increasing laminate thickness	No effect	Decreases with increasing laminate thickness
Mismatched adherends	No effect	Slight increase or decrease, depending on lay-up	No effect	Slight increase or decrease, depending on lay-up
Adhesive thickness	No effect	Increases with increasing adhesive thickness	No effect	Increases with increasing adhesive thickness
Scarf angle	Increases with increasing scarf angle	Significantly decreases with increasing scarf angle	Decreases with increasing scarf	Slightly decreases with increasing scarf angle

The effect of scarf angle on the results is important to consider, as it will determine the failure of the adhesive if the stress exceeds the maximum allowable shear or peel stress. The study also suggests that mismatched adherends have minimal effects on the overall stress. However, on observation of the results graph, it is noted that the behaviour along the bond-line has a significant amount of fluctuations from stress risers, which, under non-static, fluctuating loads, as those produced in flight, this behaviour is more likely to promote failure. This bond-line termination of the 0° fibres within the matrix produce these stress risers (Chong et al. 2018), which results in the lower observed strengths.

2.8 Failure Mechanisms

Regarding the quality of the repair, understanding the failure mechanisms and associated causation is a significant aspect. The presence of defects and bond-line stress behaviour as introduced above influence the failure behaviour and strength of the repair. Kwak et al. (2019) and Choi et al. (2016)

distinguish between the various mechanisms and propagation by means of visual inspection post mechanical testing, while Chong et al. (2018) and Chong et al. (2019) provide additional root cause analysis.
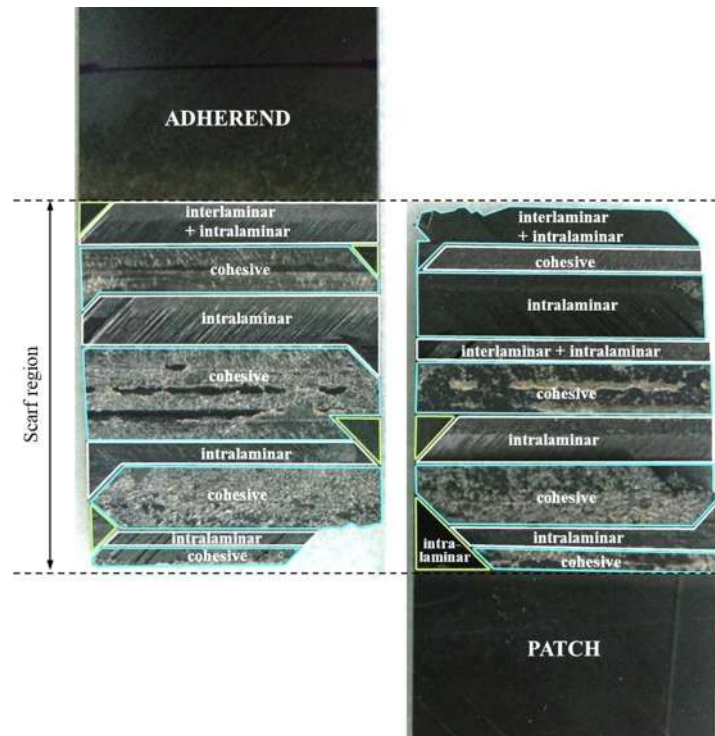
Figure 2-8: Failure mechanisms identified by Kwak et al. (2019).

As observed in Figure 2-8, the failure mechanisms identified include cohesive failure, intralaminar, interlaminar, and intralaminar + interlaminar, and is conclusive with that identified by Choi et al. (2016). For small scarf ratios of 1/10, 1/20, and 1/30, it was observed that bond area decreased as the scarf ratio decreased, with intralaminar and interlaminar failure dominant in these scenarios. This is indicative of the repair strength being close to that of the strength of an undamaged laminate (Choi et al. 2016).

The influence of adhesive distribution through the bond line was also assessed by Choi et al. (2016) and Feng et al. (2019). Figure 2-9 shows the results of microscopy conducted by Feng et al. (2019) of defects within the bond, prior to mechanical testing. The major observations include the presence of voids and uneven adhesive thickness, with variations of 130µm observed in some samples.
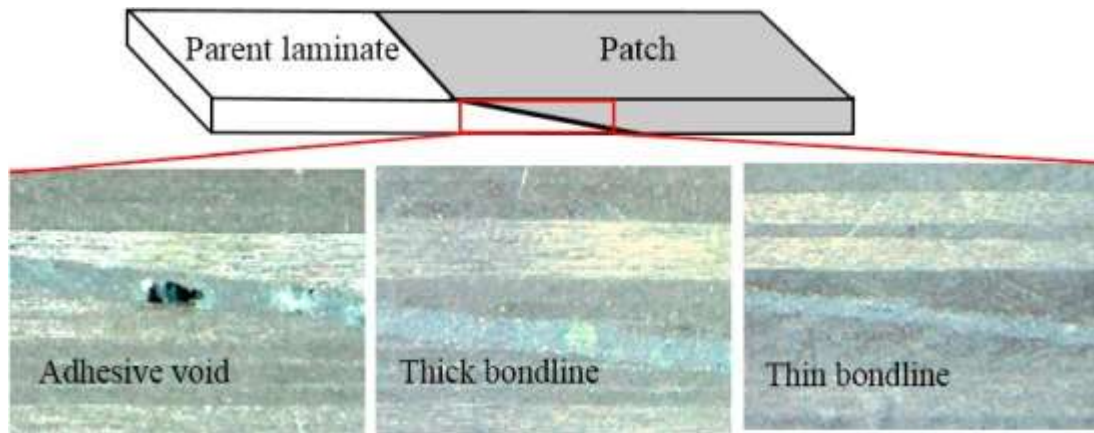
Figure 2-9: Bond-line defects as observed by Feng et al. (2019).

2.9 Machining

To ensure the quality and potential success of a repair, correct surface preparation techniques are required to ensure premature bond failure does not occur. Katnam et al. (2013) outlines CFPR behaviour such as heterogeneity, high heat sensitivity and abrasiveness, anisotropy, and low thermal conductivity adding to the complexity of typical machining processes. Various machining techniques are available, such as drilling, milling, and grinding/sanding, each with different advantages and disadvantages.

In regard to the milling technique, this was employed by Baker (2006) through the use of a 3-axis CNC process. However, due to the nature of this project and the intent that the repair be able to be carried out by non-skilled workers, and potentially without access to large industrial machines, a more typical manual process may be desired process. The method employed by the United States Navy (USN) is depicted below, which utilizes a hand-held router.

Figure 2-10: USN manual scarf machining (Baker 2006).

The manual techniques are also referenced by Duong & Wang (2005) as pneumatic routers or angle grinders, with the former being employed by Li et al. (2016). Using a die grinder with 60 and 90 grade detachable pads, Li et al. (2016) machined 2D scarf patches for their study. Another alternative which hasn't been observed in any studies is the use of a step grinder. This technique, like angle and die grinding, allows for repairs to be conducted without the need for machinery, and with tooling kits available on the market, allowing for consistent repairs. However, as suggested by the name, step grinding creates steps, rather than a smooth scarf, which introduces issues with stress risers and gaps between adhesive and corners.

2.10 Cure Modelling

Differential scanning calorimetry (DSC) is a technique used to assess the heat flow during a chemical reaction. By measuring the absorbed or evolved heat (Botehlo et al. 2005), the cure profile can be monitor, based upon the expected behaviour. Epoxy systems, as found within most carbon fibre prepreg systems, behave exothermically, releasing heat throughout their cure. These DSC measurements can then be applied to cure kinetics modelling for glass transition temperature, viscosity, and degree of cure. Chong et al. (2019) applied a viscosity comparison technique, depicted below in Figure 2-9, to demonstrate how the adhesive and prepreg behave differently under the same temperature.
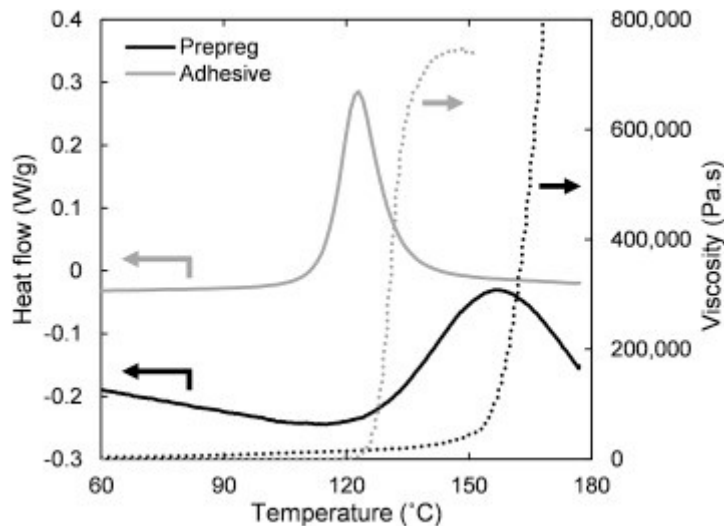
Figure 2-11: Viscosity and heat flow behaviour of adhesive vs prepreg (Chong et al. 2019).

The most significant aspect of this comparison is that the viscosity of the prepreg remains low when the adhesive reaches its highest, influencing the potential for voids to become trapped within the bondline. The DSC results compiled show that the onset cure temperature occurs at 100°C for the adhesive, while the prepreg onset cure occurs at 120°C (Chong et al. 2019). This early cure onset, in conjunction with the lower modulus temperature, limits volatile evacuation paths to through-thickness, generating non-acceptable porosity levels (Hubert & Préau 2016).

Furthermore, the use of DSC to produce a Time-Temperature-Transformation (TTT) diagram, as seen in Newcomb (2019), allows for the development of theoretical optimised cure processes. While this is seen only for an epoxy system in this study, a comparative overlap, as seen in Chong et al. (2019) would allow for an optimisation/compromise for adhesive/epoxy co-curing cycles. Kinetics Neo, software supplied by NETZCH, will allow for various cure models to be developed, based upon DSC results for both the adhesive and prepreg.

2.11 Materials Testing

2.11.1 Non-Destructive Testing

Before material removal can commence, it is imperative that the region of concern be assessed non-destructively to determine the appropriate course of action and required material removal. Assessment of damage is not always as straightforward as visible ques, with barely visible impact damage (BVID) being a significant occurrence (Katnam et al. 2013). With the potential for microscopic

damage such as fibre-matrix cracking and debonding, delamination, and fibre breakage (Katnam et al. 2013), assessment is difficult, further impacted by the unique behaviour of non-homogenous materials.

Visual inspection still has its merits, as it is an effective method to locate surface damage, and further, as well as Katnam et al. (2013) and Avedlidis et al. (2003) also making reference to the coin tapping assessment, where the tone produced indicates subsurface damage. These procedures are more applicable for pre-repair damage assessment, as they do not give visual characterization of the micro-structure of the material. More extensive tests, such as ultrasonic methods, thermography, and shearography, are more applicable for assessing porosity, resin dry and rich areas, and fibre matrix cracking or delamination.

2.11.1.1 Ultrasonic Testing

Ultrasonic assessment is a significantly used method, referenced by Avdelidis et al. (2003), Caminero et al. (2013), Katnam et al. (2013), Centea et al. (2015), and Kong et al. (2018). The general form of an ultrasonic assessment is described by Avdelidis (2003) as imparting a high frequency ultrasonic wave onto a composite material, then using the varying received signals to assess the internal defects. However, in typical direct ultrasonic assessment as mentioned above, a thin couplant layer, such as oil, is required to counteract acoustic impendence. However, the need for a couplant came be overcome using indirect ultrasonic scans, such as laser-based techniques, according to Katnam et al. (2013). This technique, employed in the Kong et al. (2018) study, requires a more expensive set-up, and for an untrained user, would be more difficult to understand than methods such as x-ray or optical micrography.

In a study by Day et al. (2013), ultrasonic C-scans were conducted on a specimen at random points, to assess laminate quality. It was implemented on DVD cured specimens, to assess if the introduction of an adjusted cure cycle had any effects when compared against the standard quickstep cycle. The below image is an extract from the study.
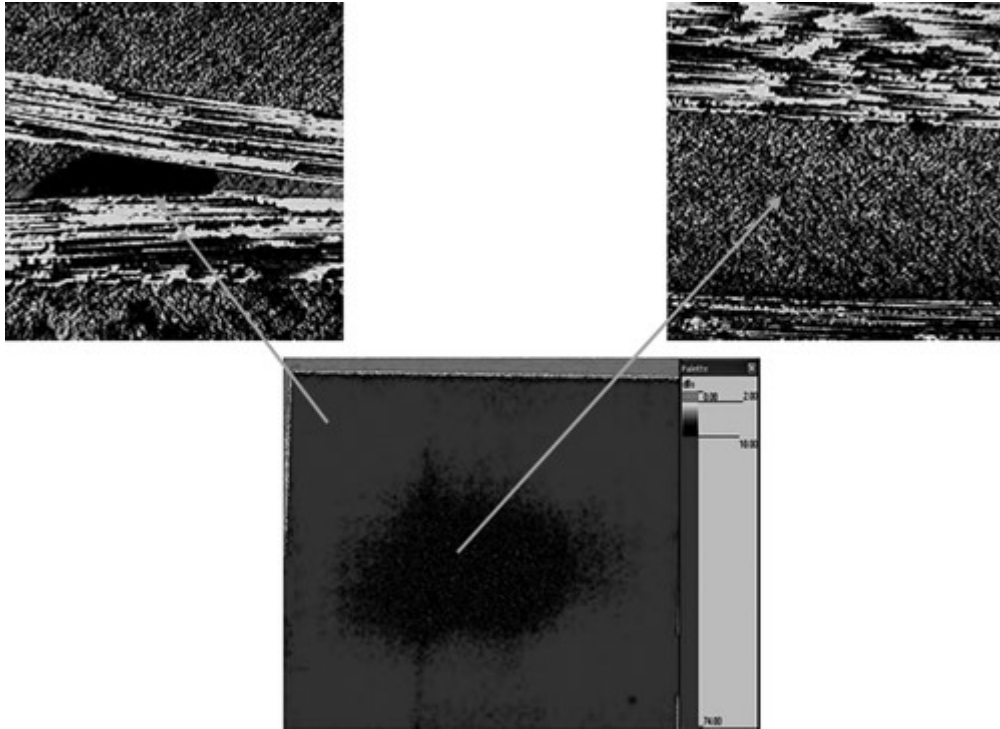
Figure 2-12: Ultrasonic C-scan (middle) with associated microscopy images (left, right) (Day et al. 2013).

It can be seen that the different shading represents significantly different microstructures. This shading is the result of the attenuation variance of the material, which, from this study, showed lower attenuation and spread for the adjusted cure cycle. It is a seemingly difficult method to understand void presence without the assistance of the microscopy images, but offers through thickn

2.11.1.2 Micro-CT

Micro-CT scanning is a more novel approach to void assessment, when compared to approaches such as Ultrasonic Testing or the Archimedes test. Alsberg et al. (2014) defines micro-CT as a non-destructive tool for producing a high resolution 3D image from 2D x-ray cross-sections. The predeceasing technique of x-ray computed tomography has seen extensive use for 50 years, mainly within the medical profession, however, the development of micro-CT over the past 20 years has seen it become more prominent in the materials sector. A significant benefit of Micro-Ct is the ability to assess the entire material, unlike micrographic imaging, and, as a result of a study by Bettini et al. (2016), micro-CT produced similar average results to that of acid digestion, which was conducted in accordance to ATM D3171.

Micro-CT has seen employment by Centea & Hubert (2011) for impregnation analysis, while also being employed by Gonzalez et al. (2019) and Jones at al. (2012) for void characterization and analysis. In the study by Gonzalez et al. (2019), micro-CT was used to assess void evolution throughout the cure cycle, under VBO conditions. This study also compared the void evolution differences of hand lay-up versus automatic lay-up, which showed a high final porosity in the hand laid specimen. This 'during cure' assessment is similar to that employed by Centea & Hubert (2011), the results of which are presented in the image below.
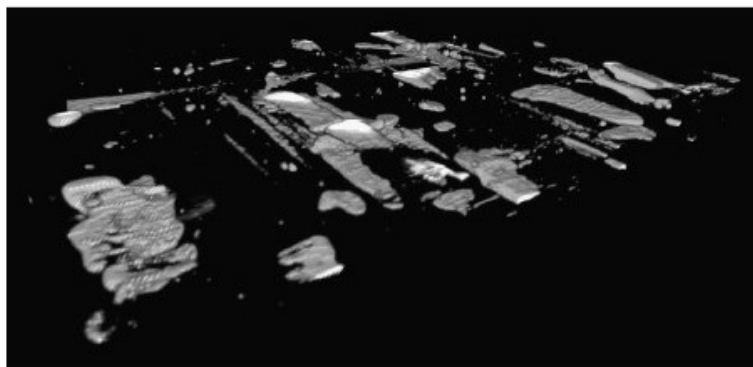
(b) LAMINATE 5 – Sample A – 60 Minutes

(c) LAMINATE 9 – Sample A – 110 Minutes

Figure 2-13: During-cure micro-CT scans depciting void content and morphology (Centea & Hubert 2011).

As can be observed in the above image, the attenuation variance caused by the presence of voids allows for a detailed 3D rendering to be formed. However, as there is no current standard for micro-CT material assessment, Jones et al. (2012) focused their study on validating its accuracy. This was achieved by introducing artificial voids of known geometry into a test specimen, the results of which showing micro-CT was accurate to within 1 voxel. The study also compared micro-CT to the Archimedes and optical microscopy, with micro-CT displaying a smaller standard deviation. Jones et

al. (2012) concluded that micro-CT be the most accurate method for assessment, as it is non-destructive and assess the full specimen.

2.11.2 Destructive Testing

Destructive testing is general carried out to determine the mechanical properties of a material, unlike non-destructive testing which is used to determine the microstructure of the material. However, destructive testing can include microstructural assessment, such as optical microscopy.

2.11.2.1 Optical Microscopy

Optical microscopy involves cutting a sample and polishing the edge, before taking an image using an optical microscope. This technique features heavily in many materials studies as a means of assessing deformities such as resin rich and dry areas and void formations. The below image from Chong et al. (2018) depicts optical microscopy images of two different cure method specimens, highlighting the appearance of voids.
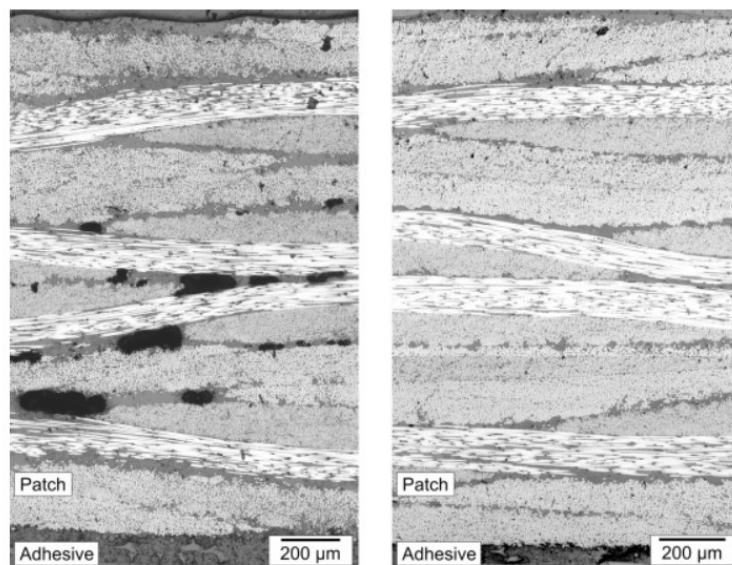
Figure 2-14: Hotbonding (left) versus DVD (right) (Chong et al. 2018).

As can be observed in the image, the presence of voids is quite easily recognized due to the easily distinguishable black areas. However, in the DVD image, the void size makes observation more difficult, thus increasing the difficulty in determining the void content.

2.11.2.2 Matrix Burnoff and Digestion

Matrix burnoff and digestion are two methods of assessing fibre volume fraction and void content, by destroying the matrix and leaving only the fibres. Bettini et al. (2016) utilise acid digestion within their studies, in accordance with ASTM D792 for density measurement of the parent specimen, and ASTM D3171 for fibre and void content. Fibre type is the overarching factor when determining matrix removal method, with ASTM D3171 (Matrix Digestion), the standard followed for carbon and aramid fibres, as they are susceptible to oxidization if ASTM D2584 (Matrix Burnoff) is followed (Mallick 1997).

Furthermore, when ASTM D3171 is utilized, it is important that the correct acid system is utilized, which is determined by the type of resin to be digested. Mallick (1997) states that there are three different acid systems, with hot nitric acid the applicable for this study, as it is best suited for epoxy resins. Over-digestion, the destruction of fibres, can occur through overexposure, so it is imperative that the correct procedures are followed, and observation is maintained throughout the process.

2.1.1.1 Tensile and Compression Testing

Tensile and compression testing are two of the most commonly utilized testing procedures for evaluating the mechanical properties, as they offer an insight into the longitudinal (and transverse, with the application of strain gauges) strength and strain of a specimen. ASTM D8131 defines the standard practice for assessing the tensile properties of tapered (scarfed) composite materials, and as such will be applicable for this study. A viable alternative is ASTM D3039, which outlines the standard tensile assessment procedures for polymer matrix materials, is closely related to ASTM D8131, and is utilized by Chong et al. (2018). These standards outline specimen size, minimum required test numbers, and other variables which must be adhered to too achieve valid results.

2.1.1.2 Flexural and Shear Testing

The assessment of flexural properties is an important aspect for composite materials, as stiffness, elastic moduli, and shear strength will vary depending on fibre orientation and material orientation. This is important to understand for aerospace and composite repairs, as loading conditions will never be purely tensile or compressive in nature. ASTM D5379 outlines the v-notched beam method for composite shear properties and has relevance for this study. Regarding Flexural assessment, ASTM D790 and D6272 are utlised by Chong et al. (2018) for assessing the flexural properties of reinforced plastics (eg. Carbon fibre) and as such are applicable for this study.

2.12 Knowledge Gaps

The culmination of the above has been studied by many, none more applicable than Hubert et al. and Chong et al. study groups out of Canada and Singapore respectively. The Chong et al. (2018) study, which has heavily influenced the preceding segments, focused on the double vacuum-debulking of the repair patch, and introduces many important concepts such as the defects and test procedures, with the Chong et al. (2019) study furthering this. This study introduces more specific results relating to the influence of the adhesive on the repair quality, while using the same approach from their 2018 study.

The porosity analysis conducted in this study was achieved using optical microscopy and micro-CT, with the latter being applied only to the parent material, and as such not offering additional insight the behaviour of the adhesive in a repair. However, the optical microscopy conducted, as observed in Figure 12, does analyse the adhesive, with a significant porosity increase (3.0% +/- 1.8% to 5.9% +/0 0.5%) observed in the SVB repair compared to the parent, while for the DVB repair, a small increase from 0.2% +/- 0.1% to 0.3% +/- 0.1% was observed for the comparative study (Chong et al. 2019).
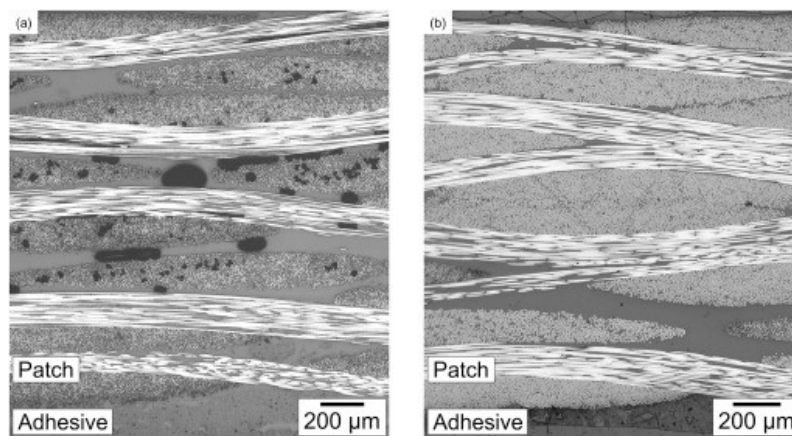
Figure 2-15: SVD repair (left) vs DVD repair (right).

The gaps observed within this study are however quite apparent. The scarf lap joint tests conducted were done using a parent to parent style, while the 2D repairs were done using a patch which was double vacuum debulked prior to being cured in the repair. The failure mechanisms observed were therefore different for the scarf and soft patch 2D repairs as well, with cohesive failure and crack propagation through the parent material observed for the scarf, while the 2D repair failure saw crack propagation into the soft patch, with no evidence of cohesive failure (Chong et al. 2019).

The influence of cure behaviour is also introduced, but somewhat overlooked. Figure 2-11 shows the cure behaviour of both the adhesive and the patch, with Chong et al. (2019) referring to the significant variation in onset cure temperature and modulus temperature, with both occurring 20°C and 30°C earlier for the adhesive compared to the patch. The implications of this are that volatiles can only undertake through thickness evacuation after adhesive patch onset cure, resulting in larger quantities of entrapped volatiles.

The 2016 and 2018 studies by Hubert & Préau were focused around porosity evolution in the bond-line with the presence of an adhesive film. The significant takeaway from the 2018 study was that higher temperatures during the cure cycle were likely to increase porosity, with higher humidity environments requiring lower curing temperatures. This study was focused solely around moisture diffusion and evolution throughout the cure cycle, and as such overlooked the effects of standard void production as a result of entrapped air.

The Hubert & Préau (2016) study, however, was tailored toward volatile evacuation throughout the cure, with the incorporation of various perforated media intermediate the adhesive and the patch. While this may not be applied throughout this study, a correlation between porosity and failure strength was identified, with further relationships between porosity and failure mechanisms observed.

Two areas of importance, identified by Hubert & Préau (2018), were the effect of cure cycle and maximising pressure distribution. These areas, in turn with the effect of single step co-curing on repair quality, will be the focus of this study.

2.13 Chapter Summary

This chapter sought to identify the overarching principles behind successful scarf repairs, namely the processing defects, techniques, and testing procedures. With significant focus currently given to the mitigation of porosity development, and comparative strength studies, it was identified that pressure distribution and effects of cure cycle had been largely overlooked. In order to reproduce successful repairs, these area require further evaluation to determine their influence on the quality of scarf repairs, more specifically in co-cured DVB repairs.

3 Methodology

3.1 Chapter Overview

To ensure the study is streamlined and accurate, it is important that an in-depth methodology be established. The purpose of this section is to establish the goals and procedures necessary to ensure an efficient and accurate study is conducted, through the use of various methods such as the creation of a focus question/s and hypothesis/es. This will be further elaborated upon through an analysis of the concept of research, and the style which this paper intends to follow.

3.2 Type of Research

The style of research utilised will determine the procedures required for an accurate study. According to Creswell (2014), research involves posing a question, collecting data, then analysing the data and answering the posed question. This is further elaborated upon by defining the style of research as qualitive or quantitative. Due to the nature of this project, with a known research question and the use of experimental data acquisition and analysis, a qualitive approach will be used. This requires defining the focus question, establishing hypothesis, and the subsequent experiment conduction and data procurement, as will be outlined in the proceeding sub-sections.

3.3 Research Focus

The focus of this research paper will be defined through; the development of research aims, outlining of the scope to be considered, and the research questions to be answered, to ensure a conclusive analysis is achieved while maintaining efficiency and effectiveness

3.3.1   Research Aim

As identified within the literature review (Chapter 2), significant knowledge gaps exist within many current research papers. There is a significant amount of research on individual concepts such as void formation and repair strengths, but research into the understanding of DVD processing of co-cured scarf repairs is widely overlooked. The main study identified, conducted by the Chong et al. study group, utilised a methodology viewed as limited, as much of the 2018 and 2019 study overlook DVD

within the cure, and merely as a means of pre-cure debulking, therefore overlooking the potential effects of the DVD on void evacuation when co-curing is carried out in one step.

The mechanical assessments conducted are also viewed as being applied in an ineffective means, as two different types of scarf repair, the scarf lap joint and 2D scarf repair, one of which is a hard patch while the other is a soft patch approach, are compared. It would be more appropriate to conduct the assessment on one style of scarf repair using the different patch approach, as this would ensure comparison of like systems is achieved.

As such, the aim of this research is to establish baseline results using a hard patch scarf repair, with which a co-cured soft patch scarf repair could be assessed against. This will ensure that relationships between the two methods are relevant, and that repair procedures are consistent throughout the study. Particularly, this dissertation will focus upon the relationship between the influence of the adhesive film on porosity evacuation and mechanical and material properties of co-cured scarf lap joints, cured using DVB methods.

3.3.2   Project Scope

Due to the brevity of this dissertation due to time constraints, requirements from DSTG, and to ensure a focused, in-depth analysis, the scope of this dissertation will be limited. The key concepts are observed in the title of this paper, with further detail provided in sections 1.3, 1.4, and 3.2.1. To summarise, the scope of the project is:

 "To analyse the bond-line behaviour and composition of co-cured double vacuum bag scarf repairs and assess the effect of pressure distribution throughout the cure cycle on final repair quality and integrity."

3.3.3   Research Questions

To ensure a streamlined study which maintains focus on the identified aim, the following research questions have been established.

3.3.3.1 Research Question 1

Regarding void formation, does the DVD process produce co-cured scarf repairs of a comparable quality to that of a hard patch approach?

3.3.3.2 Research Question 2

Are the scarf repair strengths achieved by the co-cured specimen comparable to that of the hard patch scarf repair?

3.3.3.3 Research Question 3

How does the pressure distribution vary between parent, hard patch scarf repair, and co-cured soft patch scarf repair, and how does this relate to the observed porosity and strengths?

3.3.3.4 Research Question 4

Does the presence of a caul plate influence the quality and strength of a repair specimen?

3.4 Experimental Objectives

In order to fulfil the research questions, various experiments must be established to evaluate and compare the various techniques. These experiments are focused around the destructive and non-destructive techniques considered in section 2.9 Materials Testing.

3.4.1 Non-destructive Experiments

Non-destructive testing will be used to evaluate the porosity content and distribution, particularly throughout the soft patch and bondline. This will then be compared to the parent material to determine any possible relationships between the presence of an adhesive patch, porosity content, and failure mechanisms. Microscopy will be utilised on scarf cross-sections, as it will offer insights into the bondline and height and length of porosity distributions.

An LX 205:100.100.10 X-sensor with a pressure measurement calibration accuracy of 0.5% will also be used to assess the pressure distribution of soft-patches and adhesive films, to determine if defects can be observed prior to commissioning, intended to reduce premature failure.

3.4.2   Destructive Testing

In order to determine the strength of the bonds, tensile testing will be conducted in accordance to ASTM D8131. This will ensure consistency throughout the study, ensuring all results are valid. Post testing visual inspection, through basic eye observations and photography will also be conducted to document failure mechanisms and relationship to initial failure initiation and ultimate failure.

3.5 Chapter Summary

Identified within this chapter was the methodology that will be implemented to fill the identified knowledge gaps. The research aims outlined highlight the focus of the research, which is the how the presence of an adhesive film in a soft-patch repair affects the microstructural quality and mechanical performance of the scarf repairs. The means of assessing this relationship was identified within the experimental objectives, which will be further elaborated upon and developed in the proceeding section.

4 Experiment Outline

4.1 Chapter Overview

The purpose of this chapter to outline the experimental procedures for both composite panel fabrication and material property testing. This includes detailing of SVB and DVB manufacturing processes, scarf machining technique, and the destructive and non-destructive material testing. These will be justified against the research questions posed in section 2.3.2, as well as evaluated with regard to current available literature.

4.2 Composite Panel Specifications

The materials and layup utilised for the composite panels were specified by Defence Science and Technlogy Group (DSTG) and remained consistent regardless of curing technique. The prepreg system used within this research project was a Cycom 5320-1 system, which is a toughened epoxy with increased out-life, designed for primary structures. More precisely, a Cycom 5320-1 unidirectional (UD) system was chosen. This is a military grade prepreg system specifically designed for OOA processing, while performing as well as typical autoclave systems.

This prepreg system was laid up in a [45/0/0/-45/90]3s pattern. This means the first 3 lamina were laid in this manner, with the final 3 being laid opposite, thus achieving a laminate which is symmetrical about its centre axis. The use of the 45° plies being the outer most ply supports the observations of Gunnion & Herzberg (2006) and Chong et al. (2018), which saw that the presence of 0^0 plies at the outer most layer induced stress risers, and subsequently lower material strengths.

4.3 Composite Handling

The introduction of volatiles such as moisture and particles in increased through improper handling and has undesired effects on the quality of the composite. Fernlund et al. (2016) and Grunenfelder & Nutt (2010) have both studied the effect of moisture absorption, which has significant effects on porosity for OOA cured specimens, and as such must be limited with proper handling techniques.

 As prepregs are stored frozen, there is the potential for moisture absorption during defrosting. This is mitigated by leaving the prepreg to defrost in ambient conditions, while still sealed within a plastic bag. The defrosting can then be observed as the outer bag produces moisture, which, when dry,

suggests the prepreg has defrosted and can be removed. If the defrosting process isn't complete, the hydroscopic nature of the epoxy resin system will cause moisture to diffuse into the prepreg sheets, which, due to the lack of compaction pressure available during OOA curing, the compaction pressure won't exceed the vapour pressure and porosity will form.

Andrulonis et al. (2018) from the National Institute for Aviation Research outline the repair process for bonded composite repairs of Cycom 5320-1 test panels, reference the use of non-contaminating gloves for prepreg handling. This was adhered to with the use of powder-free nitrile gloves for all prepreg interaction.

4.4 Specimen Production

The curing techniques used within this project include SVB and DVB curing. For the parent panels, DVB was utilised to produce the highest quality panel possible, while SVB and DVB were used for comparative analysis of the bonded scarf repair. The layup procedures and cure cycles for each technique, and the manufacturing process for the scarf repairs, are outline in the subsequent subsections.

4.4.1   Tooling Plate Preparation

Before layup commences, the tooling plate must be prepared to remove volatiles and ensure the cured composite panel can be removed from the surface. This requires the use of a mould remover and a release agent, with a Loctite Frekote 710-NC release agent (Appendix C) and Marbocote Mould Cleaner being used. General PPE including latex gloves, goggles, and a respirator mask are to be worn at all times when handling these chemicals.

Applying the mould cleaner is the first step in the surface preparation. A microfibre cloth is used, with the whole tooling surface cleaned with several passes. If there are still visible contaminants which don't release from the chemical, scrap carbon fibre is used to scrape the surface clean, before an additional cleaning pass is conducted. This is lastly wiped with a lint free wipe aircraft grade wipes used.

After the surface is deemed contaminant free, the mold release agent is applied, with the steps outlined as follows:

- Step 1: Apply coat with a lint free wipe only to area where the composite panel will be place. Ensure coat is applied evenly, wiping in only one direction.
- Step 2: Allow coat to dry for five minutes at room temperature.
- Step 3: Buff off layer with a lint free cloth.
- Step 4: Repeat steps 1 to 3 until a minimum of 3 layers have been applied.
- Step 5: Apply a final coat, allowing 30 minutes to cure at room temperature.

Once completed, the panel can be placed on the tooling surface and the bagging procedure can begin.

4.4.2   Bagging Procedure

For both SVB and DVB curing, the bagging procedure is consistent for laying the first bag, with the variation occurring for the DVB method after the first bag has been sealed. The materials required for the bagging, as outlined by Andrulonis et al. (2018) are:

- Sealant tape,
- Non-perforated release film,
- Nylon vacuum bag,
- Polyester breather, and
- Caul plate (optional)

Additional requirements include the hotbonding console and associated components.

Depicted below in Figures 4-1 and 4-2 respectively are the SVB and DVB procedures. As previously mentioned, the inner bagging procedure for the DVB curing is the same as that for the SVB, with the external incorporation of the rigid box, breather, and vacuum bag and port resulting in the second vacuum. When a caul plate is used, it is positioned between the release ply and breather, for both SVB and DVB.

Rigid Box

Vacuum Port

Parent | Patch/Parent

Vacuum Bag
Breather
Release Film
Tooling Plate
Heat Blanket
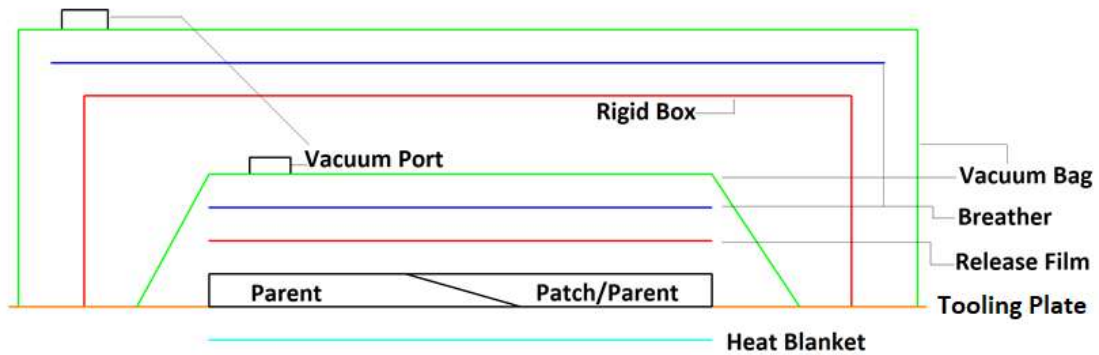
Figure 4-2: DVB layup procedure.

Figures 4-3, 4-4, and 4-5, show progressive stages of the bagging procedure, with additional details regarding materials and accessories.

Release Film

Thermocouple (fixed with high temperature tape)
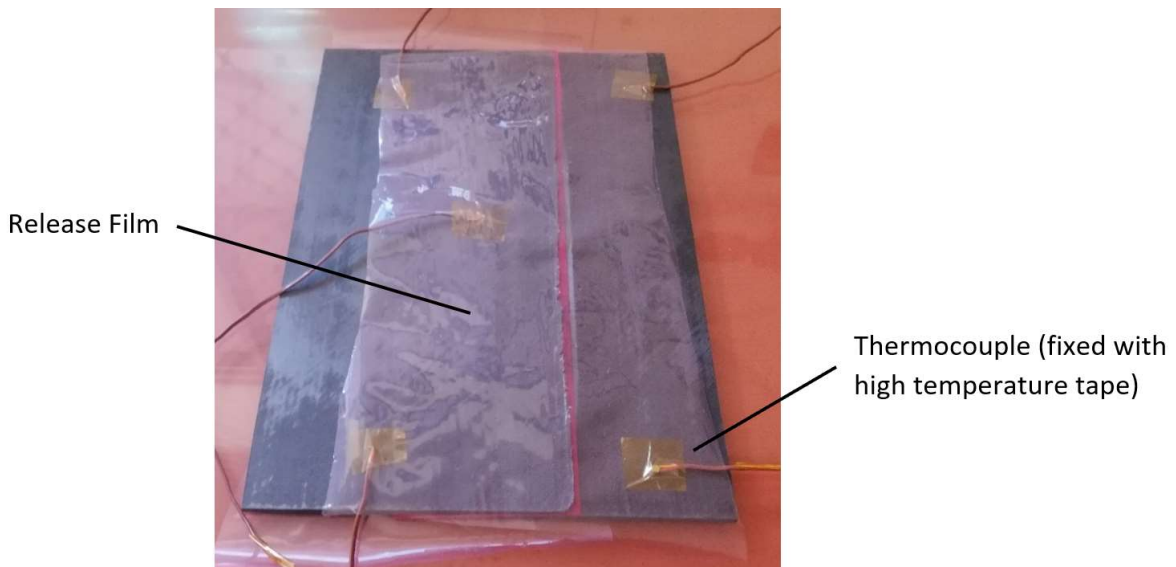
Figure 4-3: Matched repair specimen, with thermocouples fixed to upper surface.

Figure 4-3 shows the initial step, where a specimen (panel or repair), is placed on a prepared tooling surface, and thermo couples are attached with high temperature tape. For uncured specimens, such as co-cured repairs, thermocouples are attached either to the tooling plate, or only to the cured hard patch.

The next step is application of the first vacuum, depicted below.
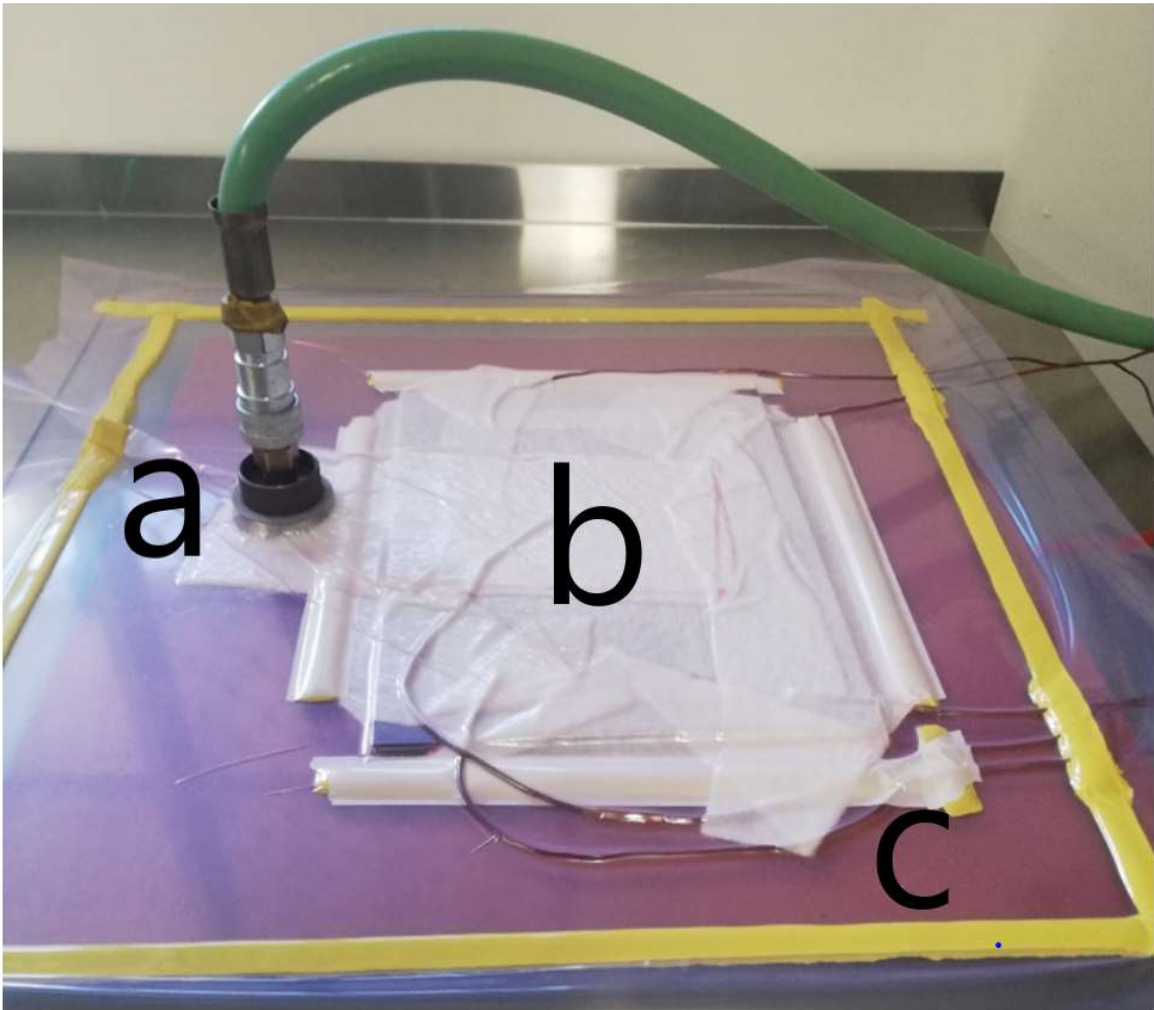
Figure 4-4: SVB specimen, with all required components, including a) vacuum port; b) breather cloth; and c) sealant tape.

Figure 4-4 above shows the final stage of the SVB procedure, with breather, sealant tape, and vacuum bag all required. Sealant tape is placed around the edge of the specimen, which the breather is placed under slightly, ensuring the specimen doesn't move during curing. A double layer of breather is placed under the vacuum port and is in full contact with the specimen to ensure successful volatile evacuation. It is also seen that the thermocouples have sealant tape above and below along the sealed edge, to ensure a successful vacuum is always applied.

Finally, for the DVB specimens, the rigid box and outer vacuum are applied, depicted below in Figure 4-5. After the first vacuum is bag is sealed, the rigid box is placed on the first vacuum bag, with a large

piece of breather placed over the top, before a smaller glass plate is finally placed on top. This is then all sealed within a final vacuum bag.
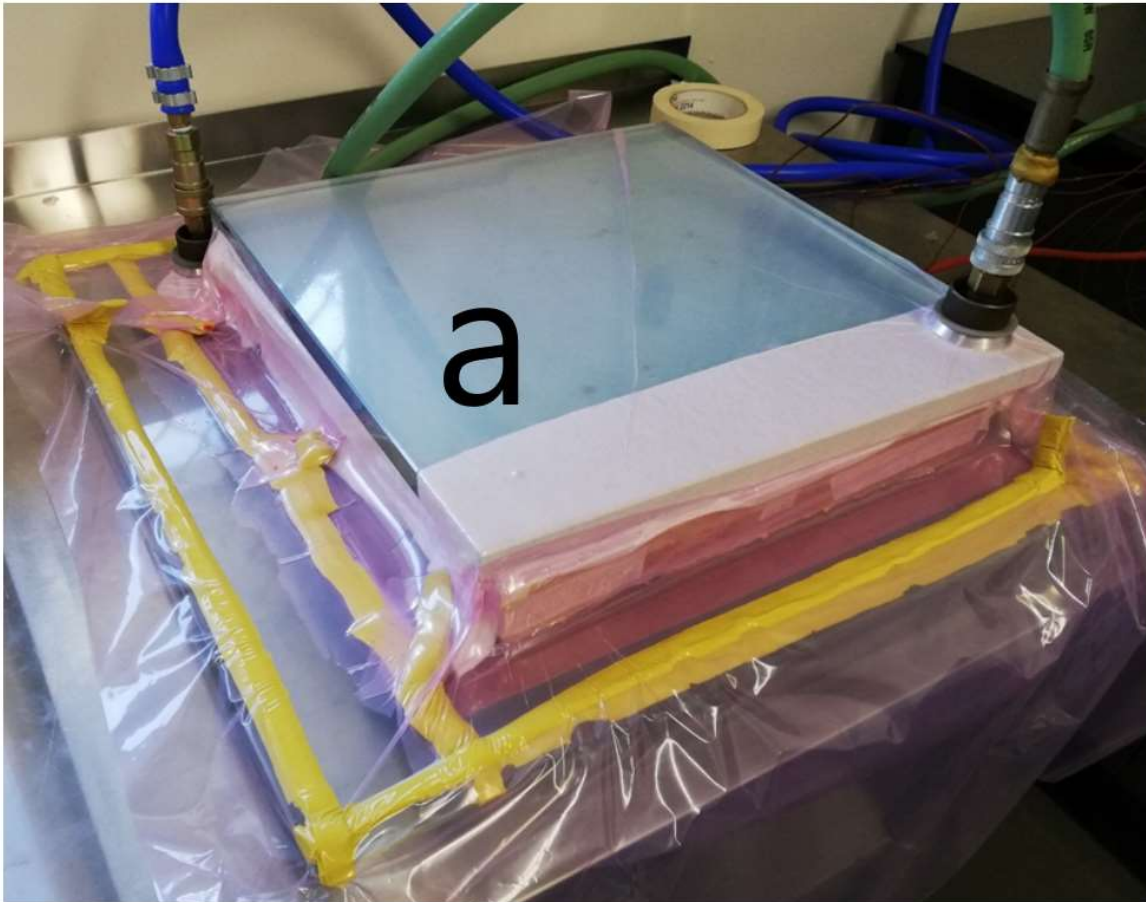
Figure 4-5: DVB vacuum set up, with all components, including a) rigid outer box.

Of interest in the bagging procedure is the use of pleating seen in Figure 4-5. Loosely applying the bag and using pleats in the seal ensure the bagging doesn't stretch and a more even compaction is achieved. It is especially important in the application of the outer bag. If the bag pulls too tightly over the rigid box, the sealant tape often stretches or releases from the tooling plate causing problems with the vacuum.

4.4.3   Cure Cycles

Both the Cycom 5320-1 prepreg and FM300-2 adhesive are designed for out-of-autoclave curing at a temperature of 121°C, with an additional 177°C post cure required for the prepreg. These were all conducted at a ramp rate of 1.7°C/min, with variation between SVB and DVB being seen in the initial stages, with the DVB incorporating a low temperature hold. This initial hold period, as previously mentioned, allows for the volatiles to be evacuated while the resin viscosity is low, and the panel is placed under no compaction pressure. Figure 4-3 shows the cure cycle for the DVB method.
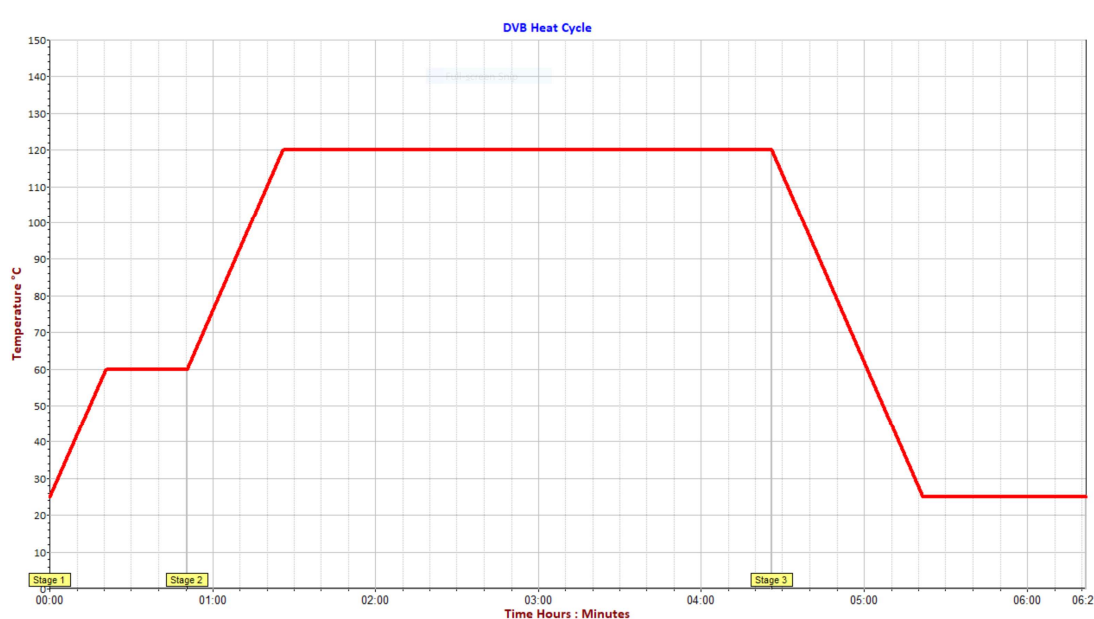
Figure 4-6: DVB Cure Cycle

The various stages of the cure cycle, as denoted in Figure 4-6 are:

- Stage 1: Under double vacuum, ambient to 60°C at 1.7°C/min, hold for 30minutes.
- Stage 2: Outer vacuum is released; therefore panel is placed under consolidation. Ramp from 60°C to 121°C at 1.7°C/min, hold for 180minutes.
- Stage 3: Release from 121°C to ambient, under natural conditions.

For the SVB curing, Figure 4-7 below depicts the cure cycle used. As previously stated, the SVB procedure follows the same 1.7°C/min ramp rate but doesn't include a low temperature hold. This is seen with the Stage 1 ramp from ambient to 121°C, with a 180min hold, followed by the Stage 2 release to ambient under natural conditions.

Aforementioned, all previously uncured prepreg specimens are then post cured in a vacuum oven for 3hrs at 177°C in a vacuum oven. For the hard patch specimens, there was no post cure after adhesive bonding, however, for the co-cured specimens, the adhesive was exposed to this post cure. As will be discussed in the proceeding chapter, this had no statistical effect on the bond strength.
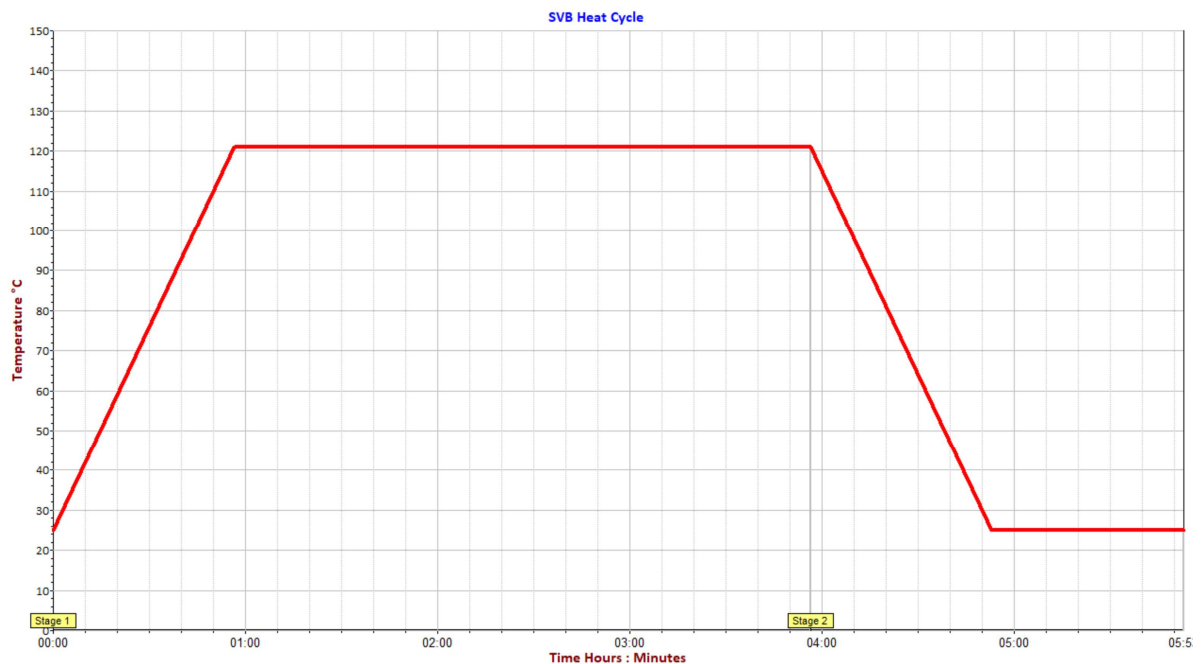
Figure 4-7: SVB Cure Cycle

4.4.4   Panel Machining

The machining of the 3° scarf was outsourced to LSM Advanced Machining for this project. 3D drawings, developed in Autodesk Inventor, were supplied for the milling. The milling was achieved using end milling, with a Kennametal KCN05 bur router (Appendix D). It is important to note that the machined edges resulted in the scarf running parallel with the 0° plies, which in theory results in lower strengths when tensile testing is conducted.

4.4.5   Scarf Surface Preparation

To ensure the bonding is correctly achieved, DSTG provided surface preparation procedures which were applied for all scarfed surfaces. The steps required for surface preparation are:

1. Under running water, sand with 400grit aluminum oxide paper.

2. Using aircraft grade wipes, wipe surface with methyl-ethyl-ketone (Appenidx D) based mould cleaner until no more particles are picked up. Wipe only one direction, using a clean wipe each pass.

3. Use distilled water to conduct a break water test. If surface performs correctly, dry with aircraft grade wipes.

4. Dry at 110°C for one hour in a vacuum oven to ensure surface is dry and dust free for bonding.

5. Remove from oven and allow to cool to ambient temperature.

4.4.6   Patch Layup

To produce the co-cured patches, the first step was to determine the length of each ply, based upon the number of plies, and the angle and length of the scarf. These calculations are presented below.

$$L_{scarf} = t_{\frac{panel}{\theta_{scarf}}}$$

(3)

The theoretical values for the panels, thickness, t_{panel}= 3.9mm, and scarf angle, θ_{scarf}= 3°, gave a scarf length, L_{scarf}= 74.42mm. This number was then divided by 30 plies to determine the length at which each ply was offset from the previous, calculated at 2.48mm (approximated to 2.5mm). To ensure sufficient length for both bonding and mechanical testing, the largest ply length was decided upon at 150mm, with the smallest ply being 75mm long. In order to maintain a uniform edge, a 2.5mm wide measured piece was placed over the preceding ply, with the new ply butted into this surface.

4.4.7   Repair Layup

For the repairs, a few variations for the adhesive were considered. Andrulonis et al. (2018) recommending an overhang over each side, as seen in Figure 4-8, which, after pressure mapping (Chapter 5), was reconsidered with no overlap and offsetting the adherend from the scarf edge to compensate for the adhesive thickness. In all scenarios, the adhesive was matched to the scarf surface, with the soft-patch then matched accordingly. This was then cured according to the procedures outlined in 4.4.1, 4.4.2, and 4.4.3.

Figure 4-8: Initial adhesive overlap, which was reconsidered after pressure mapping.

4.5 Pressure Mapping

As outlined in Research Question 3, in an effort to understand the bondline behaviour of the specimens, pressure mapping was conducted prior to curing, on a fully prepared repair. Using a high resolution LX205:100.100.10 X-sensor, the pressure distribution throughout the scarf body could be evaluated, showing regions of high pressure, low pressure, or uneven distribution. Figure 4-9 below shows the setup used for the pressure mapping.
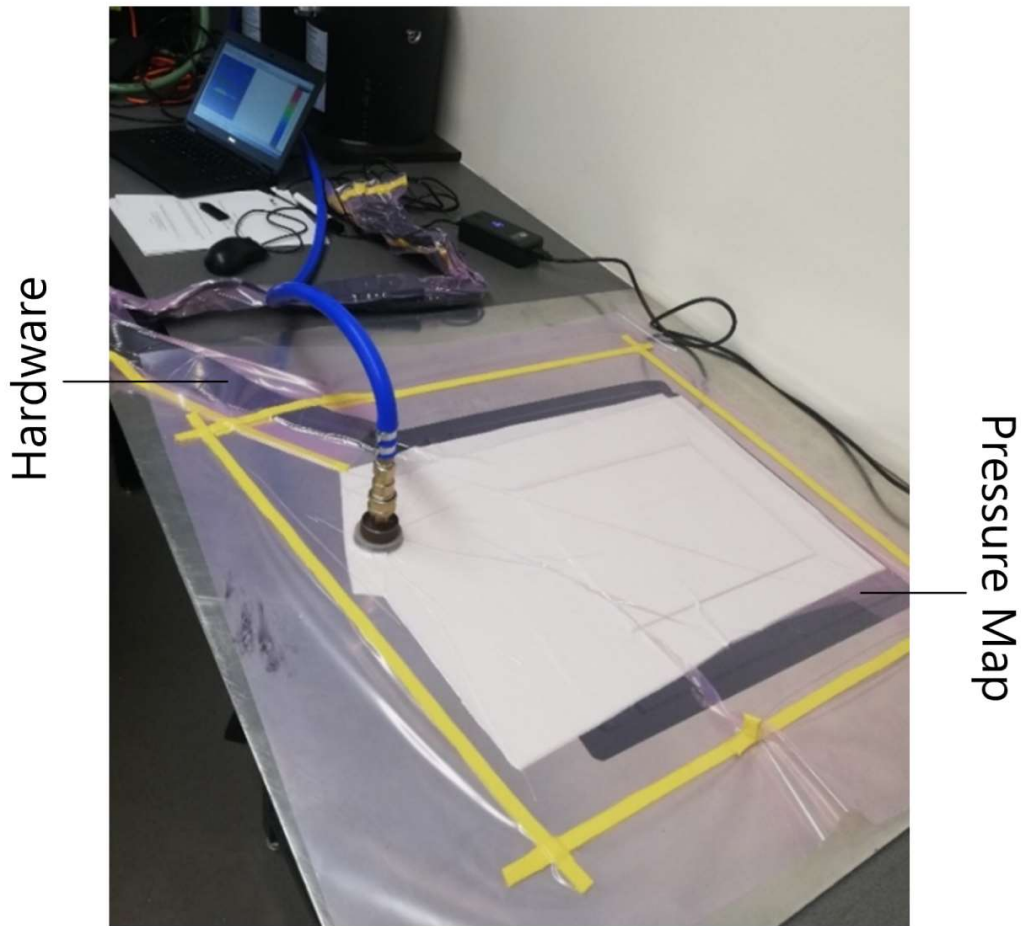
Figure 4-9: Pressure mapping setup.

This set up uses the same bagging as the SVB method seen in Figure 4-1, with the difference occurring with the removal of the heat blanket, and the inclusion of the pressure mat intermediate the tooling plate and the repair specimen. As observed in the Figure 4-9, additional difficulty is seen with the bagging procedure, as the connection hardware for the sensor pad must also be vacuum bagged.

4.6 Tensile Testing

In order to answer Research Questions 1 and 2, it was proposed in Section 3.3.2 that destructive testing be conducted. This was achieved through the use of tensile testing via a 100kN MTS Insight testing rig, as seen in Figure 4-9. The large panels were first cut into 1inch wide specimens using a diamond table saw, being numbered to relate the specimens back to their position within the whole panel. This was done to determine any potential relationships between failure mechanism/porosity development to the pressure distribution. As mentioned in section 4.4.4, the orientation of the fibres resulted in the tensile load running through the 90° plies, as depicted in Figure 4-11.

Figure 4-10: MTS Insight 100kN test rig w/ specimen.
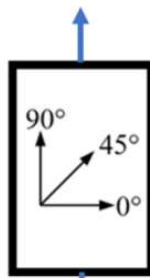
Figure 4-11: Fibre orientation respective to tensile loading.

To conduct the tensile testing, the following procedure was employed:

- Step 1: Cut panel into 1inch strips, numbering to maintain position within the whole repair.
- Step 2: Adjust grips to correct height and set loading rate to 1mm/min.
- Step 3: Measure width and thickness through scarf body with digital callipers, recording data in excel spreadsheet.
- Step 4: Insert specimen into loading rig and perform test.
- Step 5: Record failure load in excel spreadsheet.
- Step 6: Report steps 2 to 5 for all remaining specimens.

It was noted in Chong et al. (2019) that measurements for width and thickness were taken through the parent material and not the scarf body, however, it was deemed more appropriate to take measurements through the scarf body, to get a conservative strength value given the greater area through the scarf, than to take measurements through the body.

4.7 Microscopy and Failure Mechanisms

After the tensile testing was completed, selected specimens were photographed to determine failure mechanisms, with microscopy being conducted on the scarf surface to determine porosity size and distribution. This is in line with techniques outlined in Section 2.8, in fulfilment of Research Questions 1 and 3. In order to quantify the quality of the bond, a Leica optical microscope was used on the failure surface, to photograph the porosity present. These images were then analysed with ImageJ to determine the size of the porosity. This data was the used to determine porosity percentage, size distribution, and to observe any potential relationships to the pressure distribution.

4.8 DSC Testing

The procedures followed to conduct the DSC testing were done in conjunction with those outlined by Newcomb (2019) and Botelho et al. (2005). This required proper specimen handling procedures as outlined in 4.3. A _____ machine was used for DSC testing, which required specimens of approximately 10mg to be assessed. These specimens were individual weighed and recorded before being placed and sealed within a T-zero aluminium pan. An empty T-zero aluminium pan was also sealed, used as the reference specimen for the tests. To ensure a holistic assessment of the material

cure properties, three heating rates, as observed in Botelho et al. (2005) were assessed: 3; 5 and 10 ^{o}C.min^{-1}. The data computed was then exported as a plain text file, ready for importing into the NETZCH Kinetics Neo software for cure modelling.

4.9 Chapter Summary

Identified within this chapter were the experimental procedures undertaken to ensure the identified knowledge gaps and subsequent research questions were fulfilled. Significant focus was given throughout to proper handling and surface preparation procedures to ensure that volatile introduction was thoroughly mitigated. The outsourcing of the panels for machining meant quality control was more difficult to monitor but allowed for correct tooling machinery and pieces to be utilised. The challenges encountered throughout the manufacturing and testing experiments will be presented in the proceeding chapter.

5 Results

5.1 Chapter Overview

This chapter presents the results from pressure mapping, mechanical testing, visual inspection, and cure modelling work. The results and observations are then, when appropriate, compared against those seen in literature, to assess their validity, and if any additional relationships are present.

It must also be noted that sample size varied between 7 and 10 samples, which was a result of initial manufacturing defects which required material removal. Appendix E contains all recorded data for measurements and tensile testing.

5.2 Pressure Mapping

The first experiment assessed was the pressure mapping, which was identified as a novel qualitative approach for assessing the relationship between processing technique and porosity development. This was outlined in Research Questions 3 and 4, with the procedure then developed through Section 4.4.5. The results of the pressure mapping are presented chronologically, with their influence on the progressive manufacturing process used detailed throughout.

5.2.1 Adhesive Overlap Variations

The first assessment utilised the adhesive overlap identified by Andrulonis et al. (2018) and was conducted without a caul plate. As seen below in Figure 5-1, pressure distribution throughout the repair is poorly distributed, with high pressure regions observed throughout the adhesive overlap, and low pressure seen throughout the scarf body.
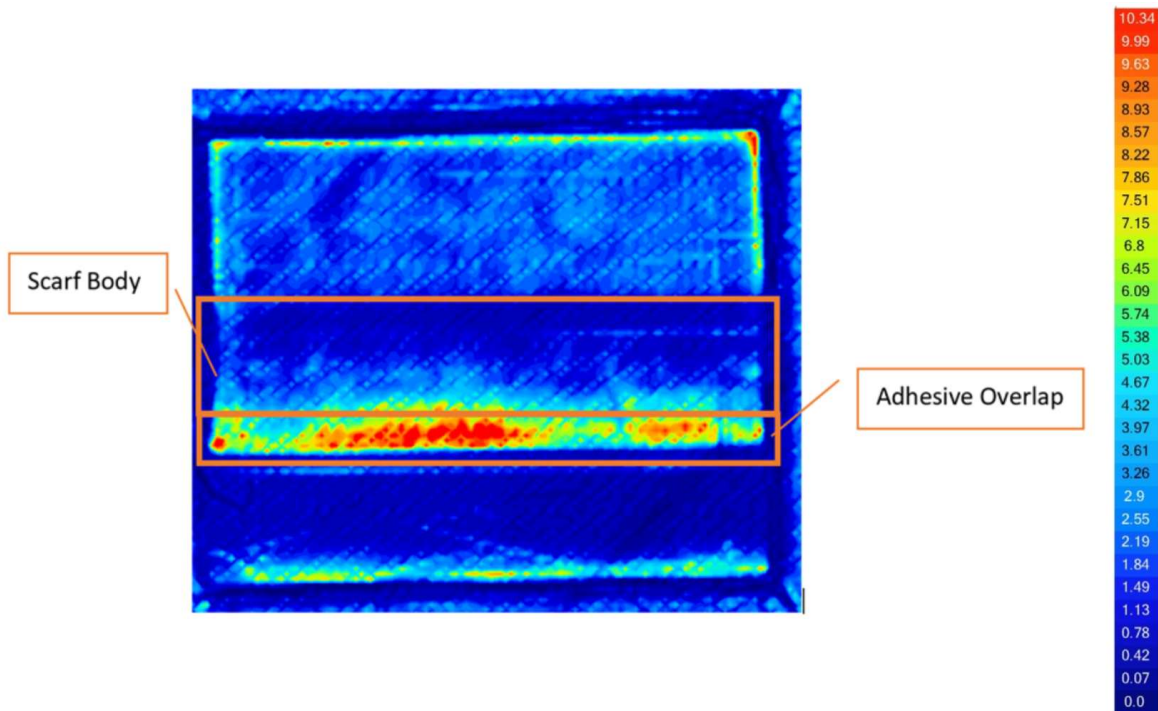
Figure 5-1: Soft patch repair with the recommended adhesive overlap (with 10 KPa scale).

For the next consideration, as above, the adhesive overlap was maintained, however, the soft patch scarf edge was offset from the parent scarf edge by 5mm (3 ply edges) as a means of accounting for the additional thickness offset caused by the adhesive. The pressure mapping results for this technique are seen in Figure 5-2 below.
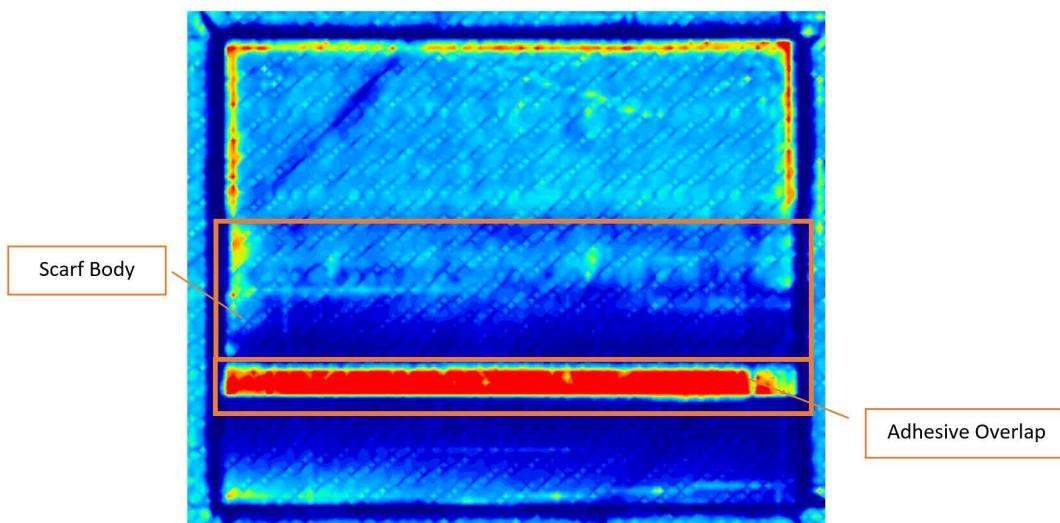
Figure 5-2: Adhesive overlap with offset adherend.

Much like that observed in Figure 5-1, the pressure throughout the adhesive is much higher than that of the scarf body, however, the adherend offset has resulted in a more even distribution. The initial observations of this is that the offsetting of the adherend produces more consistent pressure distribution, and more likely more consistent and higher strengths.

However, this initial observation is flawed, with a lack of consolidation pressure noted throughout the scarf body and soft patch itself. Due to minimal observed tooling pressure, the consolidation pressure observed would therefore be even more insignificant, and likely fail to supress vapour pressure.It was therefore decided for the next assessment that the adhesive overlap would be removed, and the effect of a caul plate would be assessed.

5.2.2 Caul Plate vs No Caul Plate

To assess whether a caul plate would influence the quality of the bond, pressure mapping was conducted on hard and soft patch specimens, to compare how the bond-line stress distribution varies between the two configurations. As stated above, it was decided upon after the initial pressure mapping results that the adhesive overlap would be removed to address the lack of consolidation pressure seen within the scarf body and adherend.

The first results of this, as seen below in Figure 5-3, offer a more uniform consolidation pressure within the scarf and eliminate the high stress in the adhesive overlap.
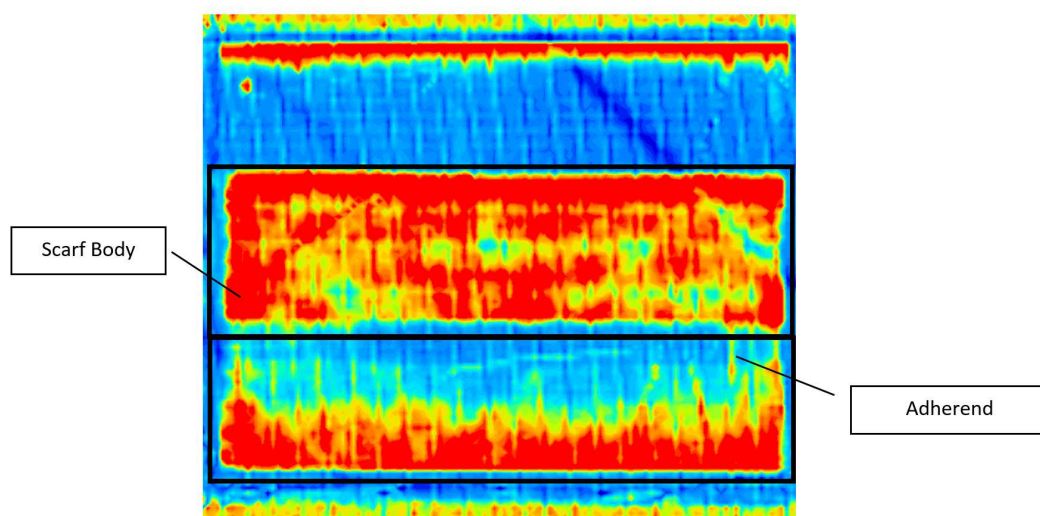
Figure 5-3: Soft patch with caul plate.

The major observation of this initial pressure mapping experiment is that the scarf body is under a significantly greater consolidation pressure than what was experienced when the adhesive overlap is present. It is important to note that this experiment included a caul plate and the removal of the overlap, and as such may overlook the interaction between overlap and caul plate.

While the body of the adherend still has regions with lower consolidation pressure, as the cure cycle progresses and the viscosity of the resin changes, it would be expected that consolidation become more uniform. This would also be influenced by the manufacturing process, with the stage 1 ramp and hold for the DVB cure providing no consolidation throughout this period.

The next experiment conducted was on the benchmark hard patch approach, comparing the effects of the caul plate, and offering a comparison for the co-cured method.
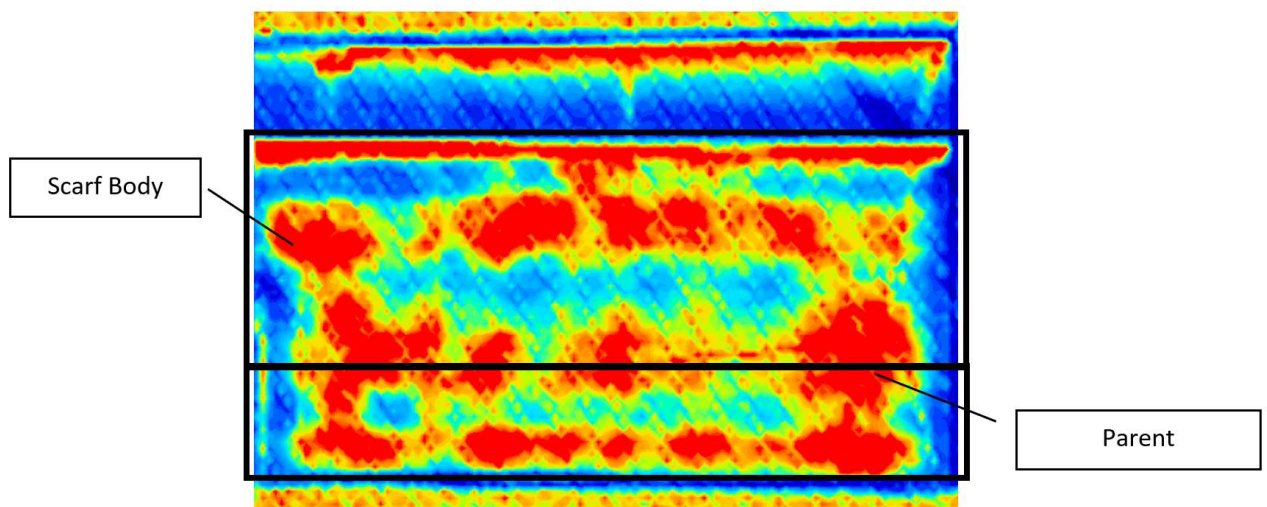
Figure 5-4: Hard patch repair without caul plate.
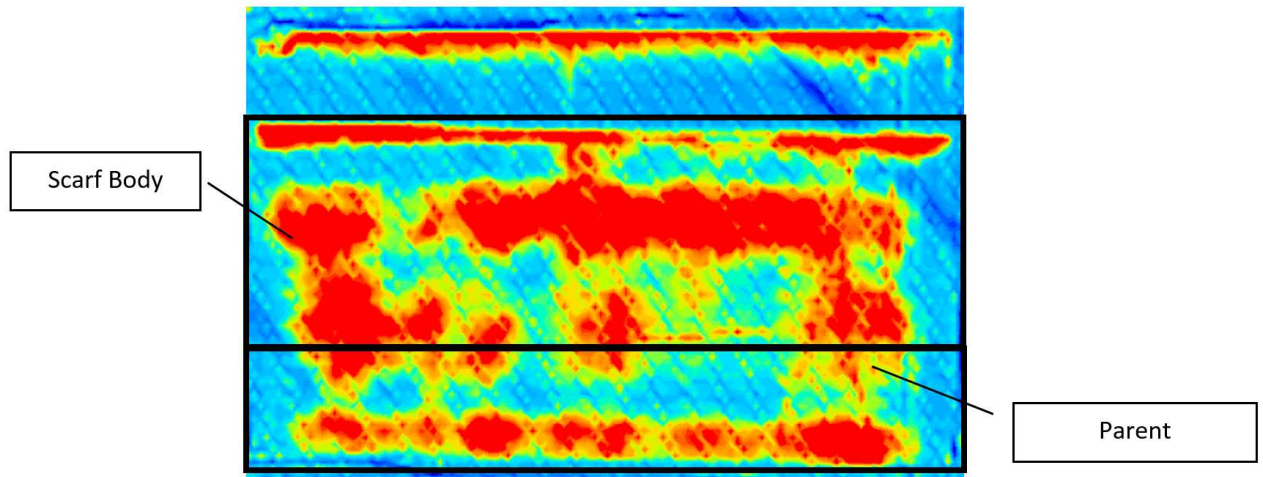
Figure 5-5: Hard patch with caul plate.

Comparing Figure 5-4 and 5-5, the inclusion of the caul plate doesn't significantly affect the pressure distribution throughout the scarf body, with the imperfections a result of the surface finish of the parent's outer bottom face. When compared with the co-cured specimen in Figure 5-3, it's seen that the pressure is less evenly distributed, as the co-cured due has a smooth outer surface, and the adherend is able to conform to the scarf surface while uncured. In this regard, it is observed that surface finish is an important factor for the hard patch approach, as the presence of the caul plate increases the effects of the poor surface finish.

As also previously stated, the lack of consolidation observed during the DVB stage 1 ramp and hold may also influence the quality of the bond, as the adhesive cure would progress without consolidation. These relationships are further explored in Section 5.4.

5.3 Thickness

To fully understand how the pre-cure pressure distribution affects the quality of the final repair, tensile testing was conducted, performed closely to the standards defined by ASTM D3039. For this testing, each panel was cut into 25mm wide tabs, and placed under tensile loading at 1mm/min. The average thicknesses with standard deviation, measured prior to each test using digital callipers, are presented in the table below.

Table 5-1: Average widths and standards deviations of specimens.

SAMPLE	AVERGAE THICKNESS (MM)	STANDARD DEVIATION (MM)
SVB HARD PATCH (BASELINE)	4.618	0.1157
SVB CO-CURE (W/OVERLAP)	4.763	0.0920
DVB CO-CURE (W/OVERLAP)	4.639	0.1097
DVB CO-CURE (W/OFFSET ADHEREND)	4.283	0.1122
DVB CO-CURE (W/CAUL PLATE)	4.360	0.0378
DVB HARD PATCH (W/ CAUL PLATE)	4.317	0.0833

Table 5-1 offers an interesting insight into dimensionality control via manufacturing process. While the adhesive had a fixed thickness, the thickness of each sample type varies, with the specimens with overlaps or without a caul plate having the greatest thickness. Comparing the two hard patch specimens, with and without a caul plate respectively, as seen in the proceeding figure, shows how the position within the panel affects the thickness, and the influence of the caul plate on thickness and dimensionality control.
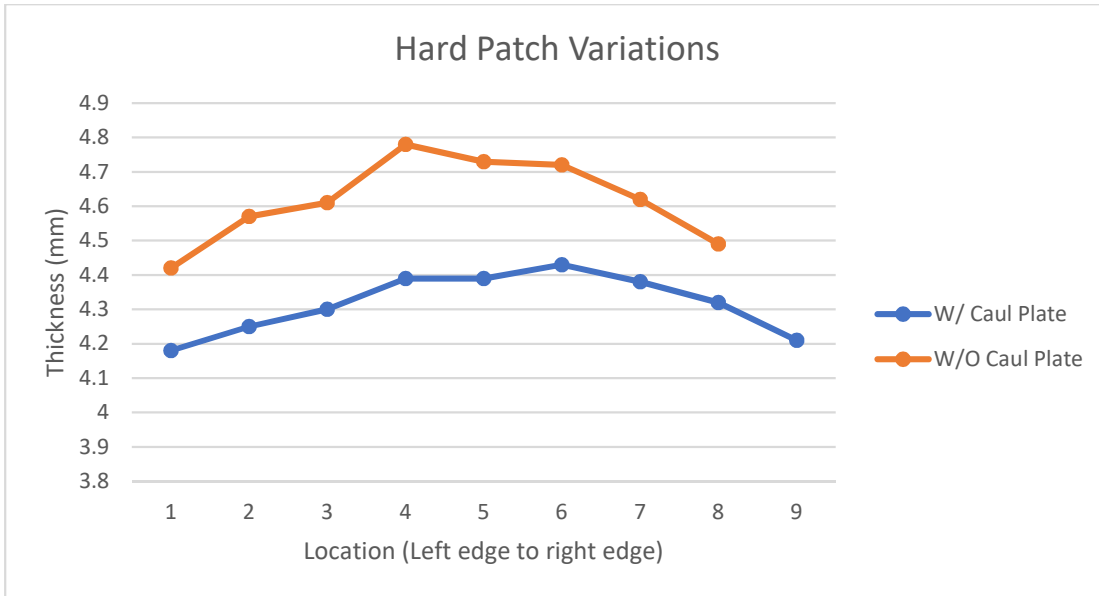
Figure 5-6: Thickness vs location for hard patch specimens.

The position within the panel, denoted by location, is as the specimens were cut from the panel. This order was numbered and maintained to help determine any further relationships which may relate to the location. As expected, the edge specimens represent the thinnest regions of the panel, as they have the greatest evacuation capabilities, as the EVaC's are unobstructed along the edge, and therefore not limited to through thickness such as the inner regions.

5.4 Tensile Testing

The tensile testing experiments were conducted on the six groups identified in Table 5-1, on a minimum of five specimens per group, except in the case of the SVB hard patch baseline, as manufacturing defects observed prior to testing limited to four testable specimens. Specimen quantity varied depending on parent size, with some panels being smaller due to manufacturing imperfections. As outlined in Section 4.6, the width and thickness of each individual specimen was recorded prior to testing to calculate the strength. A summary of the strengths and standard deviations are also supplied in Table 5-2.

Table 5-2: Strength and standard deviation of specimen groups.

Sample	AverAge Strength (MPa)	Standard Deviation (MPa)
SVB Hard Patch (baseline)	408.1	28.1
SVB Co-cure (w/overlap)	337.9	62.4
DVB Co-cure (w/overlap)	391.5	48.5
DVB co-cure (w/offset adherend)	348.4	33.9
DVB Co-cure (w/caul plate)	401.6	27.6
DVB Hard Patch (w/ caul plate)	374.5	35.2
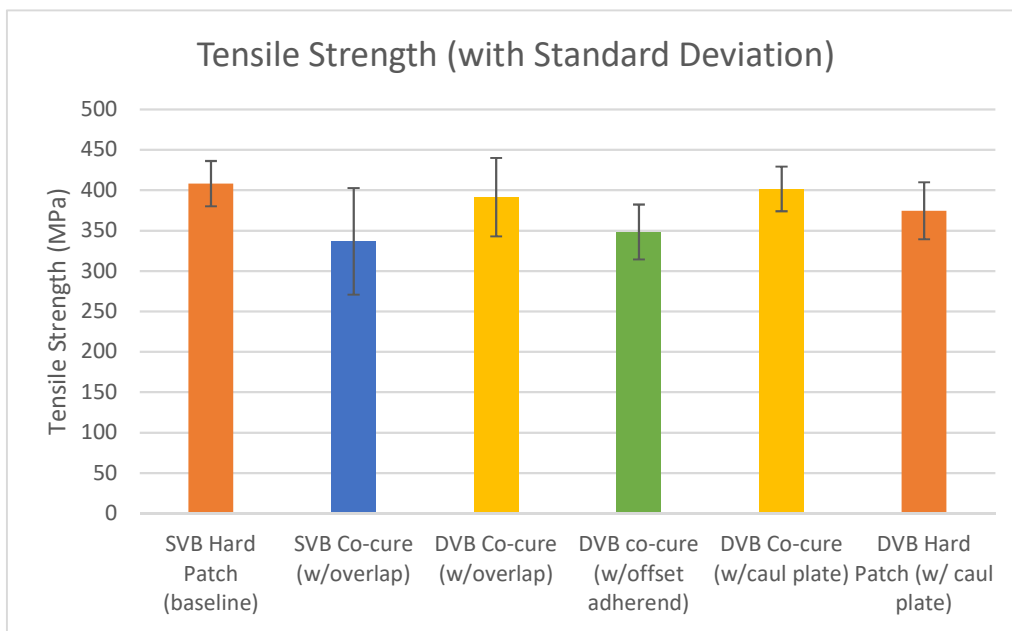
Figure 5-7: Tensile test strength with standard deviation.

As seen in Figure 5-7, the strength of the groups varied significantly, with some unexpected relationships occurring. The most notable result was the comparable strength and standard deviation of the SVB hard patch specimen and the DVB co-cured with caul plate specimen. As previously mentioned, outliers were identified prior to testing for the baseline group, with material delamination,

possibly related to coupon cutting observed on four specimens. These samples were tested but removed from the final data group, as they are a result of improper manufacturing (this group was the first attempt, and as such panel imperfections occurred). These specimens were also observed to be towards the middles of the panel, producing some of the larger thicknesses of this group, indicative of poor consolidation and high porosity.

Of all groups assessed, the DVB co-cure with caul plate performed the most consistently across strength and thickness, with the DVB co-curing process also producing the greatest individual strength of 460MPa. Highest average strength and consistency was followed by the DVB co-cure with adhesive overlap; however, this sample group displayed a large standard deviation of 48.5MPa. This large variability was not seen in either caul plate group, with comparable or greater strengths also seen for these. The most unique behaviour identified was the patch failure of the offset adherend group, with ultimate failure occurring through the bond after material failure. While this failure is not ideal, as stress transfer ceases at the patch edge and isn't transfer through to the other patch, the following stress redistribution through the patch and resulting failure indicate a successful bond has been achieved.

Additional observations were made regarding during test behaviour and ultimate failure. In accordance with Feng et al. (2019), as the load is applied, creaking noises are produced by the specimens, however, onset load doesn't indicate whether failure will be premature. Material defects observed before testing however, such as edge delamination and bond-line porosity, were indicative of premature failure, with failure mechanisms generally occurring in the form of patch failure, rather than bond failure. This is further elaborated upon in the proceeding section.

It was also identified by Gunnion & Herzberg (2006) that an increasing distance between 0° plies increases peak shear stress. Due to the loading conditions which saw the 90° plies loaded along the axial plane, they would be considered as 0^0 plies in this regard, and as such, the lower quantity of longitudinally loaded plies with increased ply spacing would increase peak shear stress and lower tensile strength.

5.5 Failure Mechanisms

The characterisation of the failure mechanisms is an integral part of validating the strength and pressure mapping results, as the bond quality and associated failure are related. The surface observations conducted using microscopy were then compared with those outlined by Kwak et al.

(2019) and Fielder (2019), to determine the overarching failure mode and contributing factors. Figure 2-8 depicts the expected failure mechanisms in a successful bond and was used to determine the failure mechanism observed post mechanical testing.

Figure 5-8 below shows the initial visual observations prior to bond-line microscopy. When compared with Figure 2-8, it appears there is a significant lack of cohesive failure, indicative of a poor bond.
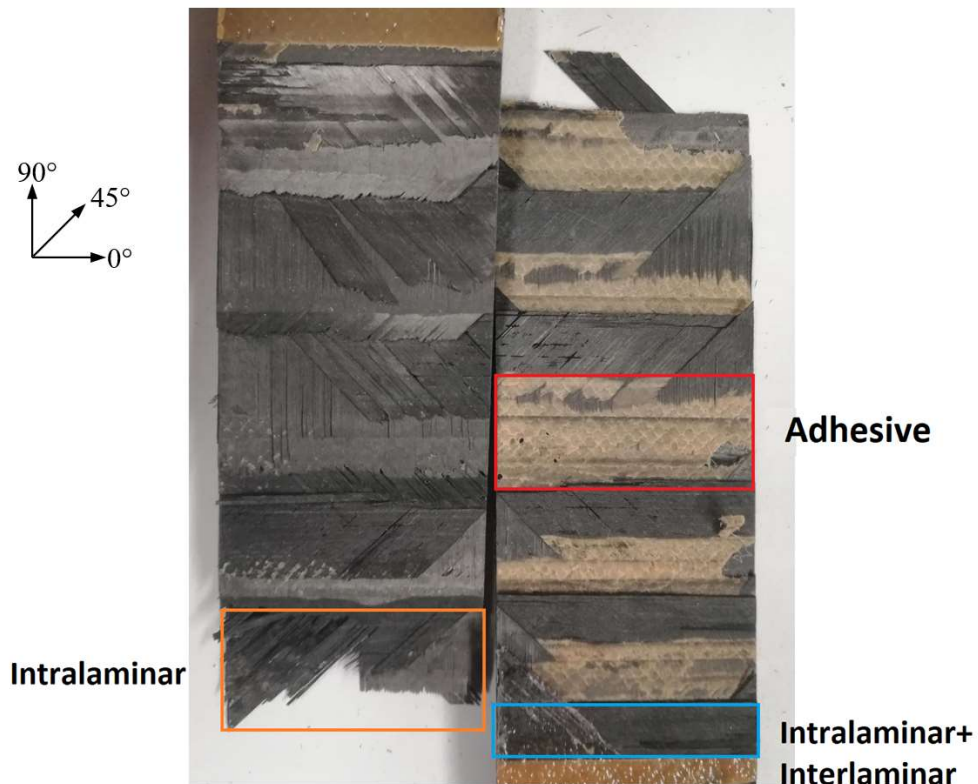
Figure 5-8: Initial failure mechanisms identified post tensile testing.

However, upon microscopic evaluation, as seen in Figure 5-9, there is indications of cohesive failure, and a relationship between porosity, manufacturing process, and failure strength is observed.
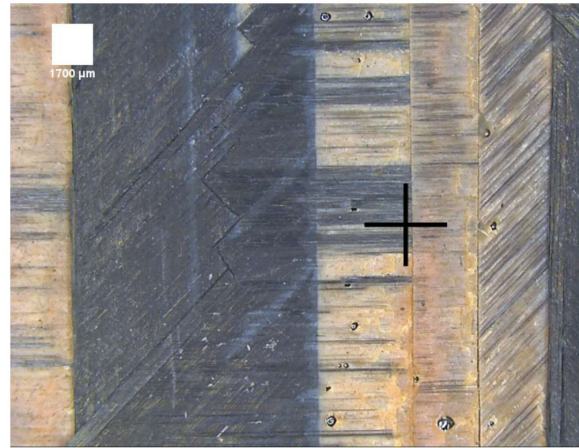
Figure 5-9: Cohesive failure seen in the form of a) large failure of reinforcement and b) yellow sheen through carbon region.

While the cohesive failure seen in yellow sheen in Figure 5-9b is less obvious than the large volumetric failure with associated reinforcement failure, both observations indicate a successful bond. The other comparison of Figure 5-9 is the porosity variation, with the bubbles seen in Figure 5-9b being from a co-cured sample. Furthermore, the below microscopic image of a DVB co-cured specimen with adherend offset coupon show significant adhesive failure, with what appears to be the development of porosity resulting in failure of adhesive-reinforcement bond.
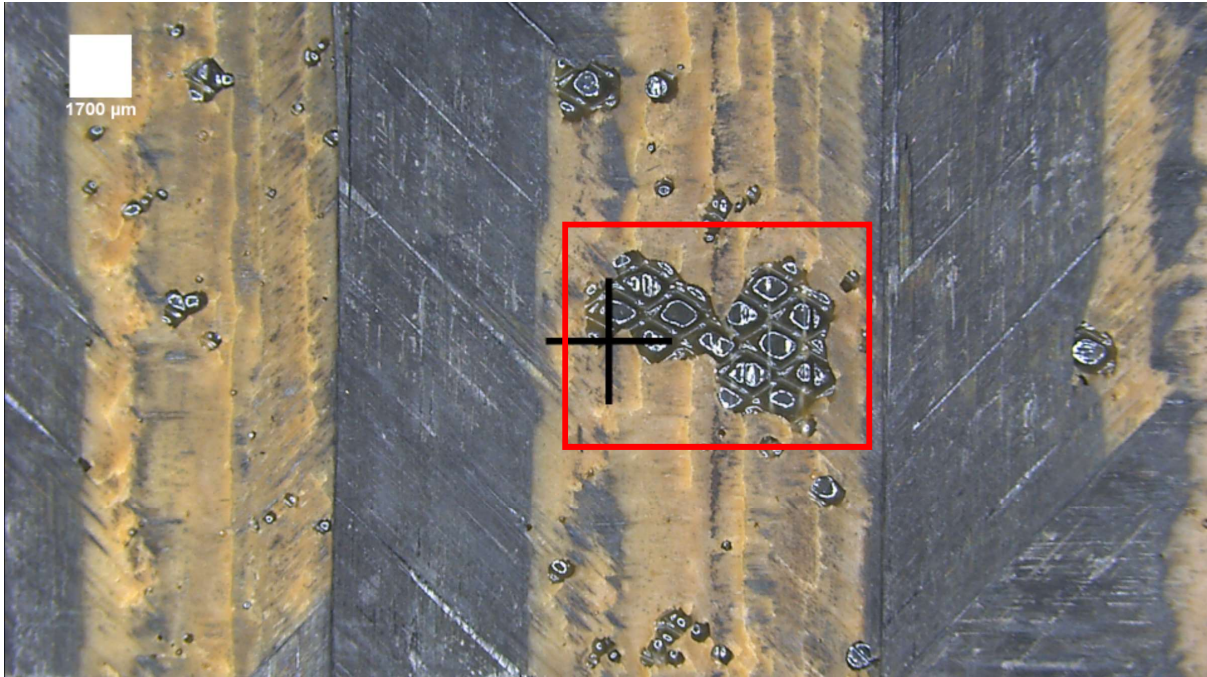
Figure 5-10: DVB co-cure offset specimen.

The large failed area, highlighted in Figure 5-10 represents an adhesive failure content of approximately 6% of the total scarf area, when analysed using imageJ software. While it may appear as porosity, when compared with the matching patch, it is an adhesive failure as this failed region is bonded to the corresponding patch. This is further demonstrated in Appendix F where a selection of failed specimens are presented.

Furthermore, for a hard patch approach, porosity levels are expected to be minimal as there is no volatile introduction through co-curing, the first repair conducted failed prematurely, likely as a result of porosity due to imperfect surface preparation. As stated in section 5.4, premature failure was observed for other specimens within this group; however, their failure is associated with pre-test material delamination, which resulted in crack propagation through the patch. Additionally, patch failure was observed within the offset adherend group, which, due to the distance between scarf edges, stress transfer ceases at the ply tip.

To further evaluate the quality of the bond line, microscopy images of selected specimens are observed in Appendix F, which have been analysed using imageJ to determine the porosity content across the 3 selected specimens. These specimens were selected based on observed quality, with a good, intermediate, and poor quality specimen selected to ensure non-biased results. The porosity content summary is presented in the following table.

Table 5-3: Bond-line Porosity Comparison for Baseline vs DVB

Sample Group	Average Porosity Content (%)	Standard Deviation (%)
SVB Hard Patch (baseline)	0.03	0.0378
DVB Co-cure (w/overlap)	0.018	0.0319

The limitations of the above evaluation is the sample size, which is currently limited to three samples per group. However, when considered with the additional images in Appendix G relationships between cohesive failure (CF), adhesive failure (AF), and cohesive substrate failure (CSF), as defined by Harder at el. (2019) and Anekar et al. (2019), are observed. Figure 5-11 below depicts the various failure forms, representative of a single lap joint under tensile loading. These failure mechanisms are a further elaboration upon those depicted in Figure 5-8.
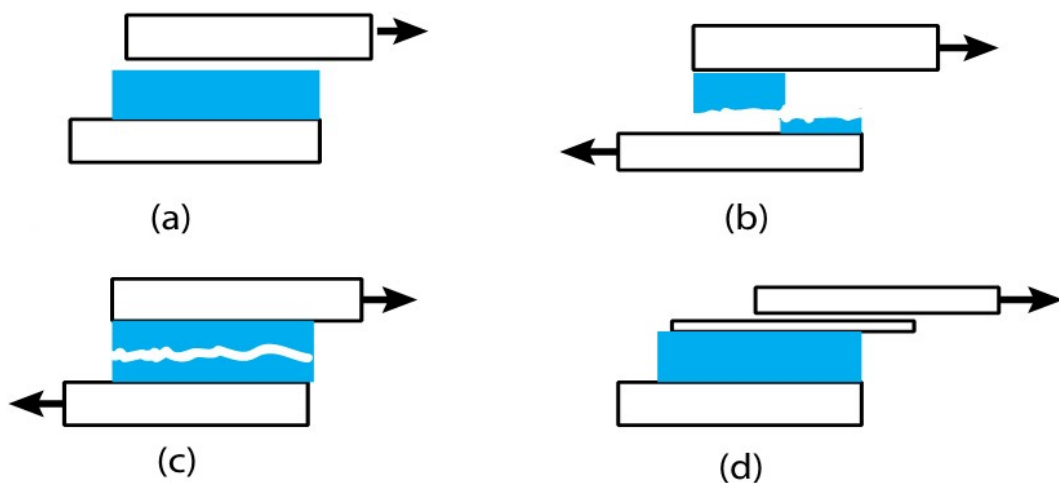
Figure 5-11: a) adhesive failure; b) mixed adhesive/cohesive failure; c) cohesive failure; and d) cohesive substrate failure (Anekar et al. (2019).

Specimens dominated by AF, demonstrated significantly lower failure strengths than those dominated by CF, CSF, or mixed CF/CFS failure. The image results observed in Appendix G are summarised in Table 5-4, with failure examples provided in Figure 5-12.
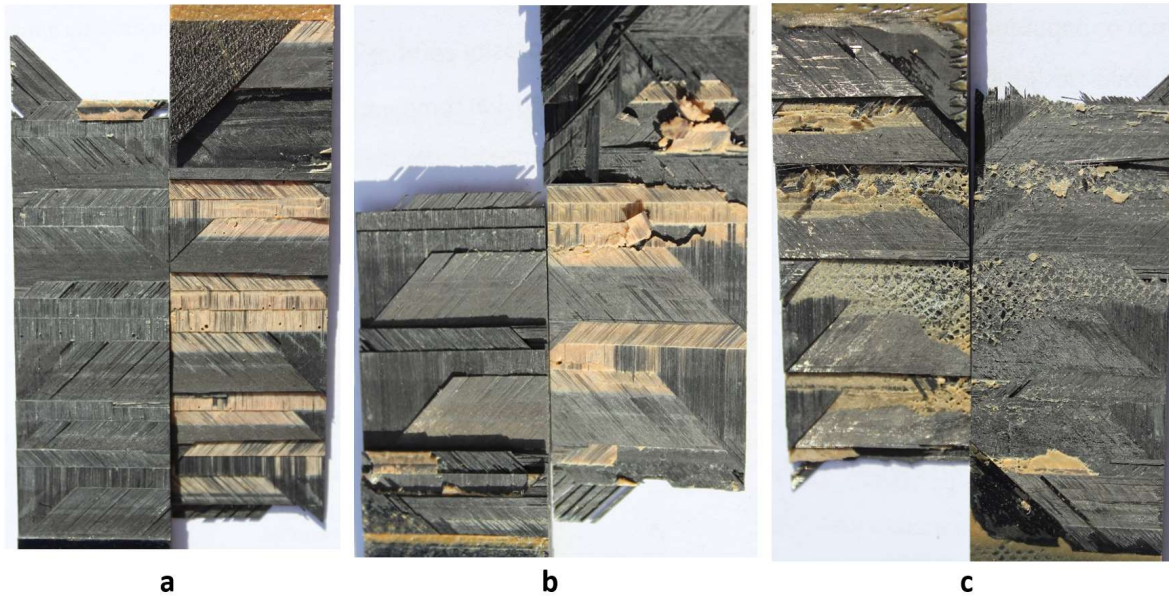
Figure 5-12: a) adhesive failure; b) cohesive substrate failure; and c) cohesive failure.

The combination of the visual assessment above and results in Table 5-4 demonstrate that when CF, CSF, or a combination of CF and CSF is present, the associated failure strength is much higher than those with associated AF. CSF was dominant for the DVB co-cured with adherend offset specimens, which was observed in tensile testing when initial failure was of the adhesive, and ultimate failure was through the adherend. The most important aspect of this test was the consistency of the failure mechanisms observed for the tests conducted with a caul plate.

The three samples assessed for the co-cured and hard patch with caul plate specimens all exhibited high levels of CF, CFS, or CF/CFS failure. CF was dominant for hard patch samples, as these samples in theory possess limited porosity due to the manufacturing conditions. However, CSF was dominant in the co-cure specimens, likely due to the manufacturing process and the interaction between adhesive and adherend under curing.

These failures do however support the observation of the pressure mapping. While the pressure mapping results were not able to identify porosity prior to mechanical testing, the improved consolidation pressure seen in Figures 5-3 and 5-5 have translated to improved consistency and quality of the bond.

Table 5-4: Failure Mechanism and Associated Strength.

SVB Hard Patch (baseline)

Specimen	Failure Strength	Dominant Failure Mechanism
1	390 MPa	CSF
3	436 MPa	AF
5	262 MPa	CF/CSF

SVB Co-Cure (with overlap)

Specimen	Failure Strength	Dominant Failure Mechanism
1	292 MPa	AF
4	415 MPa	CF/CSF
8	278 MPa	AF

DVB Co-Cure (with overlap)

Specimen	Failure Strength	Dominant Failure Mechanism
1	461 MPa	CF/CSF
4	273 MPa	AF
7	370 MPa	CSF

DVB Co-Cure (with adherend offset)

Specimen	Failure Strength	Dominant Failure Mechanism
1	412 MPa	CF
2	353 MPa	CSF
7	353 MPa	CSF

DVB Co-Cure (with adherend offset)

Specimen	Failure Strength	Dominant Failure Mechanism
1	384 MPa	CF/CSF
2	408 MPa	CF/CSF
4	384 MPa	CF/CFS

SVB Hard Patch (baseline)

Specimen	Failure Strength	Dominant Failure Mechanism
1	371 MPa	CF
3	440 MPa	CF
5	426 MPa	CF

5.6 Kinetics Modelling

To understand the impact of cure cycles on bond-line volatile entrapment, DSC experiments were conducted on the FM300-2K adhesive film at heating rates of 10, 5, and 3°C/min, with the Cycom 5320-1 prepreg being heated at 10 and 5°C/min, due to problems encountered when trying to test at 3°C/min. The results of these tests are presented below in Figures 5-12 and 5-13.
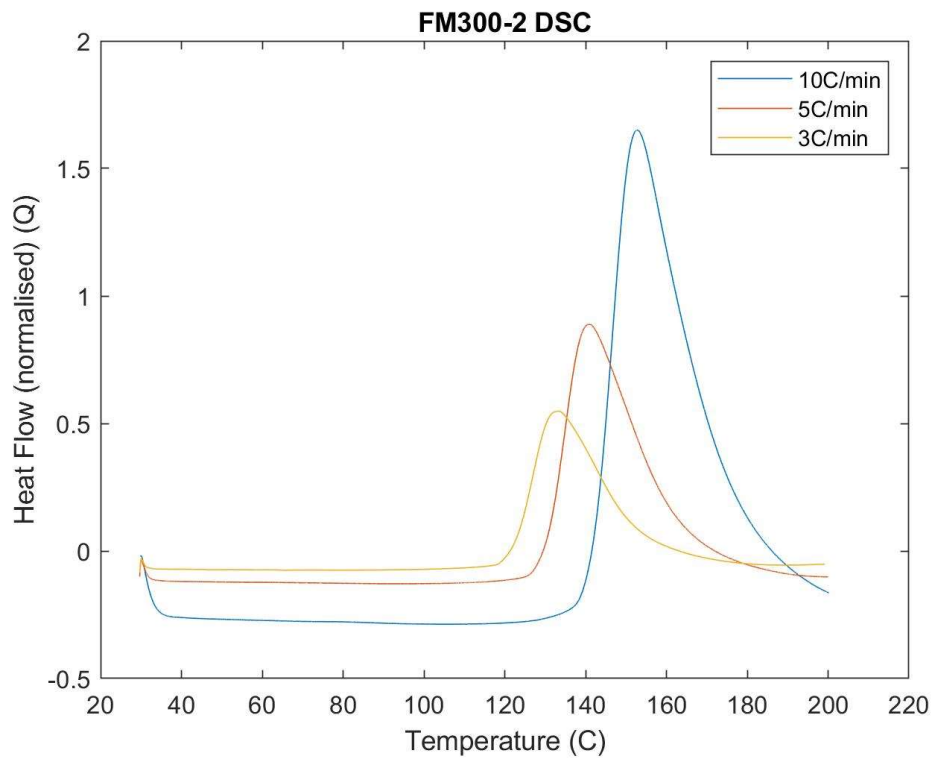
Figure 5-13: FM300-2K adhesive film DSC results.
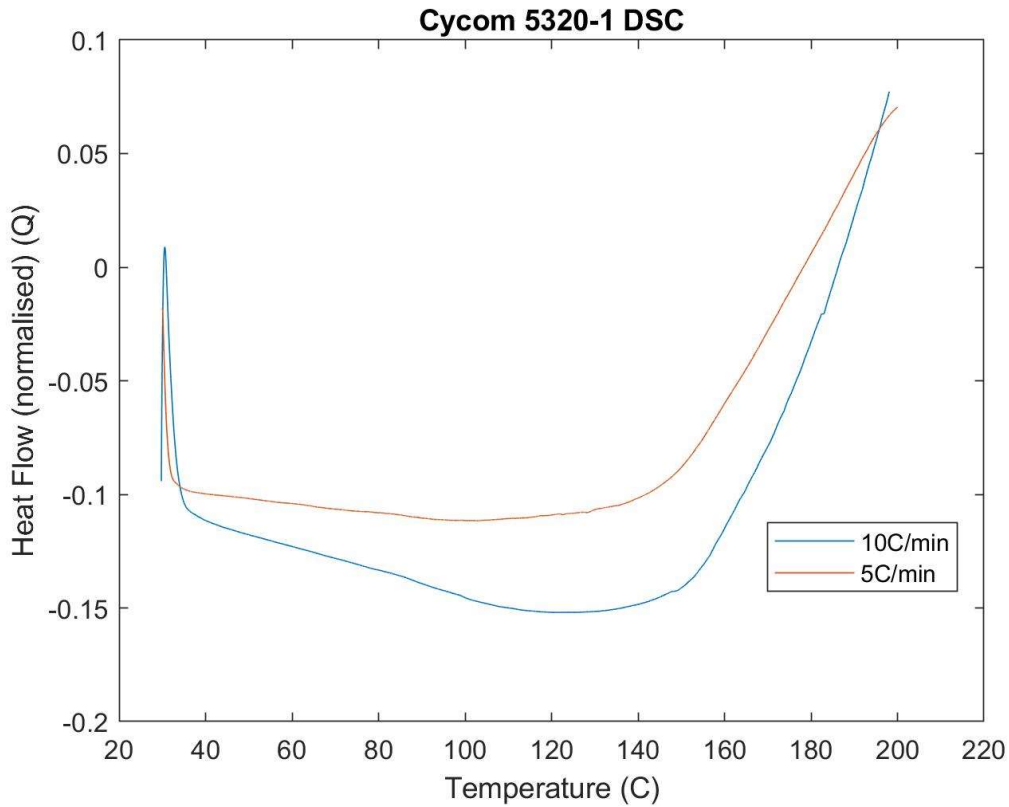
Figure 5-14: Cycom 5320-1 prepreg DSC results.

The observations from these DSC results is that while both systems are exothermic, the onset cure occurs earlier for the adhesive, with a greater normalised heat flow. These results are in conjunction with that of Chong et al. (2019) and Hubert & Préau (2016). These DSC results were then used within the NETZSCH Kinetic Neo software to produce multi-step cure predictions.

However, it is an important consideration of these models that the data correlation is done through the cure range of 100°C to 195°C of the data set, and as such, predictions outside this range must be considered tentatively. Regarding the DSC data for the prepreg, a complete cure was not seen via the DSC results, and as such, the current models are limited to the adhesive film only. The proceeding section will present the model-based predictions, while the model fitting is presented in Appendix H.1.

5.6.1   FM300-2 Predicition Models

The results presented in below in Figure 5-15 and 5-16 are the model-based multi-step cure predictions, following the SVB and DVB cure cycles respectively.
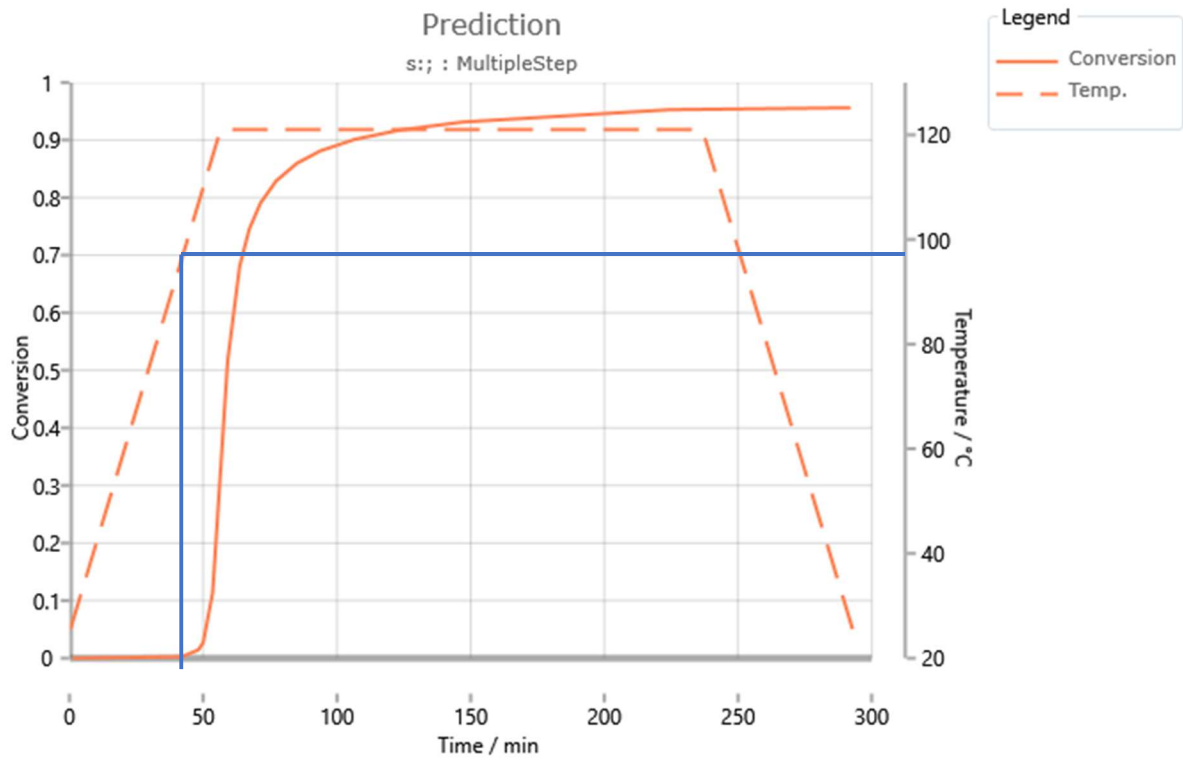
Figure 5-15: Adhesive degree of cure via SVB cure cycle (with cure onset indicated in blue).
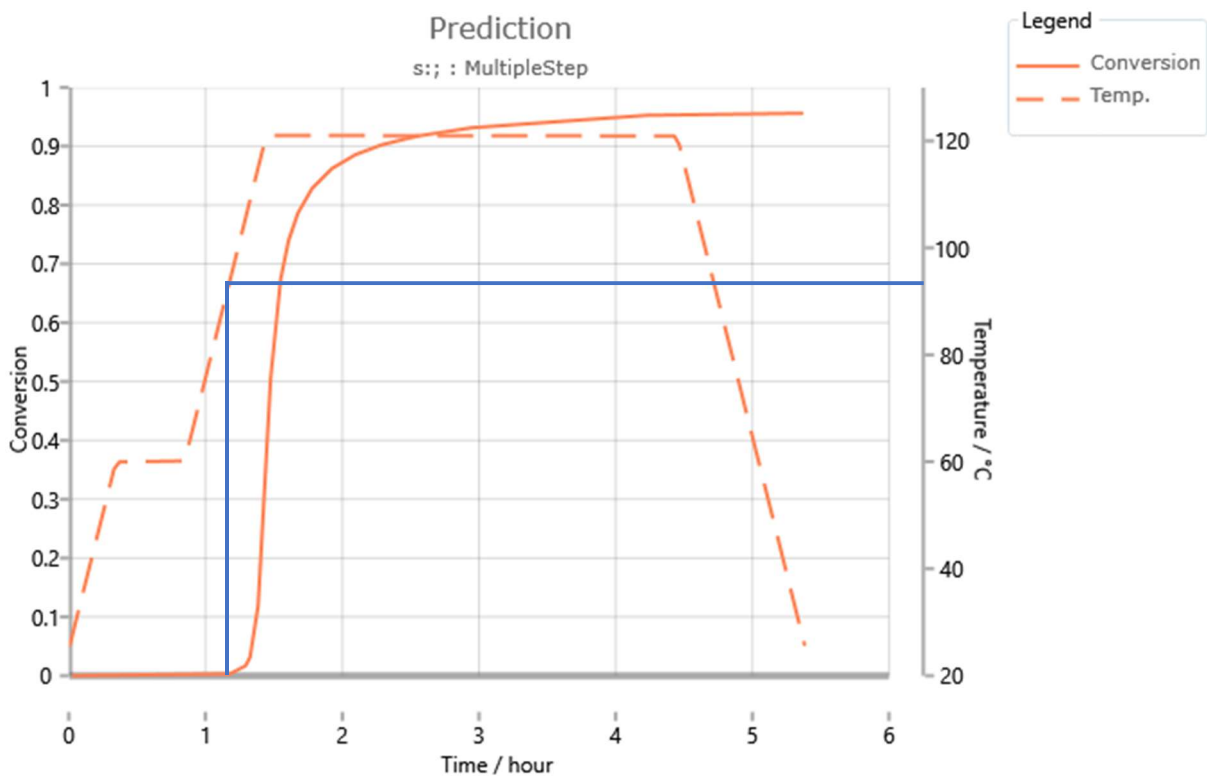
Figure 5-16: Adhesive degree of cure via DVB cure cycle (with cure onset indicated in blue).

As seen within both figures, the same degree of cure is achieved using either cure cycle, with the only delay occurring due to the DVB hold at 60°C. Without the inclusion of a carbon cure kinetics models', comparison is difficult, however, there is the potential, with further DSC testing, to produce an optimised cure cycle through conversion (degree of cure) comparison of the two systems.

With the potential for TGA assessment, glass transition temperature modelling could also be conducted, as this would offer further insight into the interaction between the adhesive and prepreg systems, and the entrapment of volatiles.

5.7 Chapter Summary

Through application of the research questions and methodology, a successful range of results were achieved, for both novel and industry practice tests. While some defects were noted, most notably for the SVB hard patch baseline, these results do not affect the study. These results will be discussed with respect to the research questions in the proceeding chapter, with the relationships between the tests expanded upon.

6 Discussion

6.1 Chapter Overview

This chapter discusses the observed results with respect to the research questions identified in Chapter 3. Relationships between the pressure distribution, porosity, and strength will be considered, with the evaluation of the available cure data and it's potential impact assessed.

6.2 Research Question 1 Discussion

Regarding void formation, does the DVD process produce co-cured scarf repairs of a comparable quality to that of a hard patch approach?

As the baseline and current industry standard, a correctly performed autoclave co-cure or hard patch repair should produce 0% porosity, as observed in Chong et al. (2019). As observed in Appendix G, basic visual inspection suggests that a high-quality repair has been achieved through both the DVB co-curing and hard patch approaches. This is further exemplified by the results in Table 5-3 and 5-4, where comparable bond-line porosity content and failure mechanisms were seen within these two groups.

Whereas the Chong et al. (2018) and Chong et al. (2019) study groups focus on the repair patch porosity, the focus of this study was the bond-line porosity, which was evaluated as a percentage of the total scarf area. The results achieved are similar to those achieved by Hubert & Préau (2016), in which bond-line porosity < 0.1% was achieved for various sample groups.

Further evaluation is required to confirm these initial observations, including the evaluation of the caul plate specimens, and the creation of additional repairs. More advanced porosity evaluation assessment is required to fully identify and quantify the porosity, throughout the patch and bond-line. Methods identified in Section 2.11 such as ultrasonic testing and micro-CT would offer a much more detailed analysis, however, these additional resources which were unavailable for this study.

The initial observations and assessments conducted throughout this study conform to the current industry observations, and as such, it is seen that Research Question 1 is successfully fulfilled.

6.3 Research Question 2 Discussion

Are the scarf repair strengths achieved by the co-cured specimen comparable to that of the hard patch scarf repair?

Summarised within Table 5-2, it can be seen that DVB co-cured specimens with a caul plate produced results comparable with the baseline specimens, however, when the DVB process was applied to the hard patch approach, it can be seen that the strength lowered and the standard deviation increased. This behaviour was unexpected and led to the assessment of the cure cycle effects on the adhesive, which will be elaborated upon in Section 6.6.

Referring back to the tensile strength of the specimens, the baseline group produced an average strength of 408 +/- 28 MPa, while the DVB co-cure with caul plate achieved 401 +/- 28 MPa. These results are in-line with those observed within literature, however, due to the thickness measured through the bond-line, unlike the parent thickness measurement used by Chong et al. (2018), these results could be interpreted as overly conservative with larger variability. The other significant observation of the strength assessment is that the repairs perform better when there is no adhesive overlap, likely due to the improved pressure distribution and bond quality.

Due to the loading direction, with the 90° plies being loaded in the tensile direction, the strengths achieved are also lower than expected if loaded along the 0° plies, with more stress risers present due to the 0° ply terminations. These should be considered further for future work, as more 'service' appropriate strengths will be achieved with these corrections.

However, as all tests were conducted under the same conditions, the comparisons conducted are accurate, and therefore, in fulfilment of Research Question 2, the strengths achieved through co-curing were comparable to the baseline hard patch, when a caul plate and DVB processing is employed.

6.4 Research Question 3 Discussion

How does the pressure distribution vary between parent, hard patch scarf repair, and co-cured soft patch scarf repair, and how does this relate to the observed porosity and strengths?

The application of this novel assessment technique offered interesting insights into the interaction of different repair techniques along the bond-line. When considering porosity, a relationship between scarf body pressure distribution and porosity content was not observed. This is largely due to the fact that each sample is consolidated under the same vacuum pressure, and porosity is predominantly

introduced through improper handling. While it was hoped that low pressure regions within the scarf body would be indicative of premature failure due to porosity, this was not observed. The major implication of the pressure mapping was the removal of the adhesive overlap, as initial investigations suggested the scarf body was largely under inadequate pressure. The improved dimensionality control was also reflected by these observations, as the caul plate introduction improved thickness, supported by the improved pressure distribution and removal of the adhesive overlap.

The failure mechanisms and strengths summarized in Table 5-4 also reflect the improved bond quality, indicative of the improved consolidation pressure achieved via the caul plate. The failure mechanisms and strengths observed are more consistent for these specimens, and as such, the application pressure mapping has led to improved quality.

6.5 Research Question 4 Discussion

Does the presence of a caul plate influence the quality and strength of a repair specimen?

As observed throughout Section 5.3 and 5.4, the improvement in strength and thickness as a result of the caul plate is significant, predominantly for the co-curing methods. The average tensile strength increase of 20MPa and subsequent standard deviation improvement for the DVB co-curing specimens, along with the 0.3mm average thickness improvement, indicate that the introduction of a caul plate successfully improved the bond quality of the specimen.

This was supported by the pressure mapping results observed in Figure 5-3, which indicated a more uniform pressure distribution throughout the bond. Studied literature did not indicate the impact of a caul plate on the quality of the repair, with Andrulonis et al. (2018) saying the caul plate was not necessary for the repair procedure. An unexpected result of the caul plate testing was decreased strength of the DVB hard patch specimen. Pressure mapping of the hard patch specimens, with or without a caul plate, showed no significant effects, rather just enhancing the impact of the surface defects. This will be further elaborated upon in Section 6.6, with the impact of cure cycle observed from this hard patch study also considered.

Overall, in fulfilment of Research Question 4, it is concluded that for the co-curing methods, the inclusion of a caul plate is beneficial, as the improved pressure distribution improved the bond quality, resulting in higher strengths and improved thickness.

6.6 Additional Observations

Identified throughout the literature review, it is noted that the adhesive and prepreg behave differently under the same cure conditions, with industry practice aware of the impact of volatile entrapment due to EVaC obstruction. Volatile entrapment through the DVB co-curing appeared to be minimal, suggesting that the manufacturing process utilised was successful. However, an additional observation of the mechanical testing, as previously mentioned, was the decreased strength of the hard patch repair, when performed under DVB conditions.

The pressure mapping results showed that the caul plate had minimal pressure redistribution affects, however, emphasised the surface deformations, which may have influenced this lower strength. However, through the application of cure modelling, it was seen that the cure onset was delayed by approximately 30 minutes when the DVB cure cycle was used, depicted in the comparison on Figure 5-13 and 5-14.

This cure cycle variation results in the cure onset occurring at a lower temperature for the DVB, but, likely due to the lack of compaction due to the outer vacuum during the initial ramp and hold, bond quality/adhesion is impacted. The variation in cure onset between adhesive and prepreg is also known to impact upon volatile entrapment during co-curing consolidation, however, due to the Cycom 5320-1 DSC data being incomplete, it wasn't able to be modelled using the NETZSCH Kinetics Neo software.

It is understood then, that the cure cycle does have considerable effects on the bond quality, both regarding porosity entrapment and adhesion success, and that the potential to apply theoretical kinetics modelling and experimental cure assessment will offer additional insights into optimising the repair procedure.

6.7 Chapter Summary

This chapter has successfully identified any potential relationships observed through the standard industry tests and novel approaches, with respect to the research questions. Furthermore, the results obtained generally conform to those observed within literature, with points of contention that require further addressing identified.

7 Conclusion and Future Work

7.1 Conclusion

The aim of this project, as defined in Section 1.3, was to assess the influence of the DVB process on co-cured scarf repairs and provide a comparative analysis against the industry standard hard patch approach. Through the establishment of project objectives and research focus questions, as defined in Section 1. 4 and 3.3.3, a holistic understanding of the behaviour of carbon fibre scarf repairs has been achieved.

Previous literature has been focused around strength and porosity comparisons and has failed to analyse the effect of processing techniques and methods which influence the quality and level of repeatability. This knowledge gap was identified, with novel approaches, such as pressure mapping and cure kinetics modelling identified as key resources to understand bond characteristics. Through the application of these novel approaches in combination with standard industry tests, the following observations were discovered:

- DVB co-curing of a Cycom 5320-1 prepreg system and FM300-2K reinforced adhesive produced results comparable to that of the industry accepted hard patch approach, regarding strength, porosity, and bond quality.
- Through the application of pressure mapping, relationships between bond quality and consistency, and dimensionality control regarding thickness were identified. The inclusion of a caul plate and removal of adhesive overlap resulted in improvements of all quantitative measurements, and perceived improvements of qualitative assessments.
- The use of the DVB method for hard patch repairs resulted in lower strengths, suggesting that the cure kinetics of the adhesive are not suited to the current cure cycle employed.

While future work, elaborated upon in the proceeding section is required to determine optimal repair procedures, the current recommendations from the above findings are:

The consolidation pressure distribution throughout the scarf body is optimal when the adhesive film and scarf edge are flush; the inclusion of a caul plate, which improves bond quality, failure mechanism consistency, and thickness control; cure kinetics modelling is conducted on both prepreg and adhesive systems, to determine the most appropriate cure cycle.

7.2 Future Work

This current study was limited due to time constraints, and as such, further investigation following the outlined procedures. The recommended future includes:

- Reconducting the DSC testing of the Cycom 5320-1, covering a full cure profile;
- Kinetics modelling of the Cycom 5320-1 cure, comparing with the adhesive cure profile, and determining a theoretical optimal cure profile for both systems;
- Dielectric cure sensing of the adhesive and prepreg using the theoretical optimal cure profile, to determine the in-situ cure behaviour;
- Retesting the DVB co-cure and hard patch tests, with larger sample sizes to determine porosity content, failure mechanisms, and failure strengths; and,
- Applying the outlined experimental procedures to 2D and 3D scarf repairs, with potential applications on complex geometries.

These outlined steps will provide a greater understanding of the cure process, and will allow for a standardised repair procedure to be developed for aircraft repairs.

8 References

Alam Khan, L, Mahmood, AH, Ahmed, S & Day, RJ 2013, 'Effect of double vacuum bagging (DVB) in quickstep processing on the properties of 977-2A carbon/epoxy composites', *Polymer Composites*, vol. 34, no. 6, pp. 942-52.

Andrulonis, R, Gilchrist, J, Lovingfoss, R, & Tomblin, J 2018, Process Specification for Composite Bonded Repair Material Test Panels using Solvay 5320-1 Prepreg, Document Number NPS 80530R, National Institute for Aviation Research, Wichita State University

Anekar, NR, Natu, AV, & Sharma, AR 2019, 'Variation of Adhesive Strength in Single Lap Joint (SLJ) with Surface Irregularities', *American Journal of Mechanical Engineering*, vol. 7, no. 2, pp. 61-7.

ASM Handbooks Online, ASM International., Materials Park, Ohio.

Avdelidis, NP, Moropoulou, A & Marioli Riga, ZP 2003, 'The technology of composite patches and their structural reliability inspection using infrared imaging', *Progress in Aerospace Sciences*, vol. 39, no. 4, pp. 317-28.

Baker, AA 1986, *Composite materials for aircraft structures*, 1st ed. edn, American Institute of Aeronautics and Astronautics, Reston, Va.

Bettini, P, Di Landro, L, Guerra S, Montagnoli F, Montalto A, Rigamonti, M 2016, 'Detection of Voids in Carbon/Epoxy Laminates and Their Influence on Mechanical Properties', Polymers and Polymer Composites, vol. 25, no. 5, pp. 371-380

Bhagwat, PM, Ramachandran, M & Raichurkar, P 2017, 'Mechanical Properties of HybridGlass/Carbon Fiber Reinforced Epoxy Composites', *Materials Today: Proceedings*, vol. 4, no. 8, pp. 7375-80.

Boerckel, JD, Mason, DE, McDermott, AM & Alsberg, E 2014, 'Microcomputed tomography: approaches and applications in bioengineering', *Stem cell research & therapy*, vol. 5, no. 6, pp. 144-.

Caminero, MA, Pavlopoulou, S, Lopez-Pedrosa, M, Nicolaisson, BG, Pinna, C & Soutis, C 2013, 'Analysis of adhesively bonded repairs in composites: Damage detection and prognosis', *Composite Structures*, vol. 95, pp. 500-17.

Centea, T & Hubert, P 2011, 'Measuring the impregnation of an out-of-autoclave prepreg by micro-CT', *Composites Science and Technology*, vol. 71, no. 5, pp. 593-9.

Centea, T, Grunenfelder, LK & Nutt, SR 2015, 'A review of out-of-autoclave prepregs – Material properties, process phenomena, and manufacturing considerations', *Composites Part A: Applied Science and Manufacturing*, vol. 70, pp. 132-54.

Chong, HM, Liu, SL, Subramanian, AS, Ng, SP, Tay, SW, Wang, SQ & Feih, S 2018, 'Out-of-autoclave scarf repair of interlayer toughened carbon fibre composites using double vacuum debulking of patch', *Composites Part A: Applied Science and Manufacturing*, vol. 107, pp. 224-34.

Chong, HM, Wu, ZA, Ng, SP, Subramanian, AS, Liu, T & Feih, S 2019, 'Influence of double vacuum debulking process on co-cured soft-patch carbon fibre composite repairs', *Composites Part B: Engineering*, vol. 168, pp. 367-74.

Composites engineering handbook, 1997, M. Dekker, New York.

Costa, M, Botelho, E, Faulstich de Paiva, J & Rezende, MC 2005, 'Characterization of cure of carbon/epoxy prepreg used in aerospace field', *Materials Research-ibero-american Journal of Materials - MATER RES-IBERO-AM J MATER*, vol. 8.

Creswell, JW 2014, *Research Design: Qualitative, Quantitative, and Mixed Methods Approaches*, SAGE Publications.

Farhang, L & Fernlund, G 2015, 'Void and porosity characterization of uncured and partially cured prepregs', *Journal of Composite Materials*, vol. 50, no. 7, pp. 937-48.

Feng, W, Xu, F, Yuan, J, Zang, Y & Zhang, X 2019, 'Focusing on in-service repair to composite laminates of different thicknesses via scarf-repaired method', *Composite Structures*, vol. 207, pp. 826-35.

Fernlund, G, Wells, J, Fahrang, L, Kay, J & Poursartip, A 2016, 'Causes and remedies for porosity in composite manufacturing', *IOP Conference Series: Materials Science and Engineering*, vol. 139, p. 012002.

Fiedler, B, Freese, J, Harder, S, Hergoss, P, Holtmannspötter, J & Schmutzler, H 2019, 'Effect of infrared laser surface treatment on the morphology and adhesive properties of scarfed CFRP surfaces', *Composites Part A: Applied Science and Manufacturing*, vol. 121, pp. 299-307.

Grunenfelder, LK & Nutt, SR 2010, 'Void formation in composite prepregs – Effect of dissolved moisture', *Composites Science and Technology*, vol. 70, no. 16, pp. 2304-9.

Grunenfelder, LK, Dills, A, Centea, T & Nutt, S 2017, 'Effect of prepreg format on defect control in out-of-autoclave processing', *Composites Part A: Applied Science and Manufacturing*, vol. 93, pp. 88-99.

Gunnion, AJ & Herszberg, I 2006, 'Parametric study of scarf joints in composite structures', *Composite Structures*, vol. 75, no. 1, pp. 364-76.

Harder, S, Schmutzler, H, Hergoss, P, Freese, J, Holtmannspötter, J & Fiedler, B 2019, 'Effect of infrared laser surface treatment on the morphology and adhesive properties of scarfed CFRP surfaces', *Composites Part A: Applied Science and Manufacturing*, vol. 121, pp. 299-307.

Holmes, M 2017, 'Aerospace looks to composites for solutions', *Reinforced Plastics*, vol. 61, no. 4, pp. 237-41.

Hou, T & Jensen, B 2004, 'Evaluation of Double-Vacuum-Bag Process For Composite Fabrication', *International SAMPE Technical Conference*, vol. 49.

Katnam, KB, Da Silva, LFM & Young, TM 2013, 'Bonded repair of composite aircraft structures: A review of scientific challenges and opportunities', *Progress in Aerospace Sciences*, vol. 61, pp. 26-42.

Little, JE, Yuan, X & Jones, MI 2012, 'Characterisation of voids in fibre reinforced composite materials', *NDT & E International*, vol. 46, pp. 122-7.

Loos, AC & Springer, GS 1983, 'Curing of Epoxy Matrix Composites', *Journal of Composite Materials*, vol. 17, no. 2, pp. 135-69.

Mouritz, AP 2012, *Introduction to aerospace materials*, Woodhead Publishing, Cambridge, England.

Newcomb, BA 2019, 'Time-Temperature-Transformation (TTT) diagram of a carbon fiber epoxy prepreg', *Polymer Testing*, vol. 77, p. 105859.

Prasad, NE & Wanhill, RJH 2017, *Aerospace Materials and Material Technologies: Volume 1: Aerospace Materials*, vol. 1, Springer Singapore, Singapore.

Préau, M & Hubert, P 2016, 'Processing of co-bonded scarf repairs: Void reduction strategies and influence on strength recovery', *Composites Part A: Applied Science and Manufacturing*, vol. 84, pp. 236-45.

Préau, M & Hubert, P 2018, 'Effects of processing conditions on bondline void formation in vacuum bag only adhesive bonding: Modelling, validation and guidelines', *International Journal of Adhesion and Adhesives*, vol. 80, pp. 43-51.

Soutis, C 2005, 'Carbon fiber reinforced plastics in aircraft construction', *Materials Science and Engineering: A*, vol. 412, no. 1, pp. 171-6.

Torres, JJ, Simmons, M, Sket, F & González, C 2019, 'An analysis of void formation mechanisms in out-of-autoclave prepregs by means of X-ray computed tomography', *Composites Part A: Applied Science and Manufacturing*, vol. 117, pp. 230-42.

Truong, V-H, Kwak, B-S, Roy, R & Kweon, J-H 2019, 'Cohesive zone method for failure analysis of scarf patch-repaired composite laminates under bending load', *Composite Structures*, vol. 222, p. 110895.

Wang, CH & Gunnion, AJ 2009, 'Optimum shapes of scarf repairs', *Composites Part A: Applied Science and Manufacturing*, vol. 40, no. 9, pp. 1407-18.

Xie, Z, Li, X & Yan, Q 2016, 'Scarf Repair of Composite Laminates', *MATEC Web of Conferences*, vol. 61, p. 05019.

Yoo, J-S, Truong, V-H, Park, M-Y, Choi, J-H & Kweon, J-H 2016, 'Parametric study on static and fatigue strength recovery of scarf-patch-repaired composite laminates', *Composite Structures*, vol. 140, pp. 417-32.

Zhan, Y, Liu, C, Kong, X & Li, Y 2018, 'Measurement of fiber reinforced composite engineering constants with laser ultrasonic', *Applied Acoustics*, vol. 139, pp. 182-8.

9 Appendices

Appendix A: Project Specification

ENG4111/4112 Research Project

Project Specification

For:	Riley Mitchell
Title:	Influence of Double Bagging Process on Out-Of-Autoclave Co-Cured Scarf Repairs
Major:	Mechanical engineering
Supervisors:	Dr. Xuesen Zeng
	Professor Peter Schubel
Sponsorship:	DSTG
Enrolment:	ENG4111 – ONC S1, 2019
	ENG4112 – ONC S2, 2019
Project Aim:	To analyse the bond-line behaviour of co-cured double vacuum bag scarf repairs, and assess the effect of pressure distribution throughout the cure cycle on final repair quality and integrity.
Programme:	Version 1, 20th March 2019

1. Research the background information relating to co-cured scarf repairs, composite behaviour, and out-of-autoclave processes.

2. Design experiments based upon DSTG specifications and methodologies observed throughout literature review.

3. Produce initial parent specimens and have sent to USQ Workshop for surface machining.

4. Conduct surface preparation and scarf repair lay-up and co-cure.

5. Conduct relevant destructive and non-destructive assessments as defined by DSTG and literature review.

6. Compile results (mechanical and microstructure properties, pressure mapping) and analyse to see if research questions are fulfilled.

7. Propose improved repair procedures, to be supplied to DSTG for continuing research collaboration with USQ.

Phase 1	Preparation Phase
1a	Project Commencement: Gain official approval from USQ
1b	Literature Review: Conduct background research and identify any potential new studies
1c	Resouce Acquisition: Acquire required resources, as outlined in section…
Phase 2	**CFRP Material Production**
2a	Produce Prepregs: Begin production of parent materials
2b	Scarf Machining: Machine parent specimens to desired scarf dimensions
2c	Scarf Layup: Layup and cure scarves for testing
Phase 3	**Destructive and Non-Destructive Testing**
3a	Non-Destructive Assessment: Conduct optical micrography and ultrasonic tests
3b	Tensile Testing: Conduct tensile tests adhering to ASTM-D3039
3c	Shear Testing: Conduct shear test adhering to ASTM-D5379
Phase 4	**Data Collection**
4a	Record non-destructive results: Record pressure mapping, micrography images, and ultrasonic results
4b	Record destructive test results: Record tensile and shear test results
Phase 5	**Results Analysis**
5a	Comparative Analysis: Compare results with other similar studies
5b	Mechanical Relationship Analysis: Assess if there is a relationship between mechanical strength and defects
5c	Processing Relationship Analysis: Determine relationships between processing parameters and defects
Phase 6	**Write-up**
6a	Draft Dissertation: Write-up and submit draft dissertation as required for ENG4111
6b	Present Dissertation: Present project background and results as required for ENG4903
6c	Final Dissertation: Submit final dissertation as required for ENG4112

Week (Commencing Semster 1, February 25th 2019)

Task/Activity	1	2	3	4	5	6	7	8	9	10	11	12	13	14	15	16	17	18	19	20	21	22	23	24	25	26	27	28	29	30	31	32	33	34	35
Phase 1																																			
1a		█	█																																
1b		█																																	
1c																																			
Phase 2																																			
2a				█	█	█			█	█	█																								
2b				█	█	█			█	█	█																								
2c				█	█	█			█	█	█																								
Phase 3																																			
3a											█	█	█	█										█	█										
3b											█	█	█	█										█	█										
3c											█	█	█	█										█	█										
Phase 4																																			
4a											█	█	█	█										█	█										
4b											█	█	█	█										█	█										
Phase 5																																			
5a																		█	█	█	█	█													
5b																		█	█	█	█	█													
5c																		█	█	█	█	█													
Phase 6																																			
6a			█	█	█	█	█	█	█	█	█	█	█	█	█	█	█	█	█	█	█	█	█	█	█	█	█								
6b																															█	█			
6c																																	█	█	█

Table 6: Proposed Project Timeline.

LOCTITE®

Technical Data Sheet

LOCTITE® FREKOTE 770-NC™

Known as 770-NC™
August 2014

PRODUCT DESCRIPTION

LOCTITE® FREKOTE 770-NC™ provides the following product characteristics:

Technology	Mold Release
Appearance	Clear, colorless[LMS]
Chemical Type	Solvent Based Polymer
Odor	Solvent
Cure	Room temperature cure
Cured Thermal Stability	≤400 °C
Application	Release Coatings
Application Temperature	15 to 60 °C
Specific Benefit	• No contaminating transfer • High gloss finish • High slip • No mold build-up • Low odor

LOCTITE® FREKOTE 770-NC™ offers excellent release for various molding applications. LOCTITE® FREKOTE 770-NC™ can be used for the release of epoxies, polyester resins, vinyl ester resins, thermoplastics, adhesives, and rotationally molded plastics. This product is particulary well suited for tougher to release processes such as filament winding and non gel coated polyester and fiberglass molding.

TYPICAL PROPERTIES OF UNCURED MATERIAL

Specific Gravity @ 25 °C   0.715 to 0.725[LMS]

Flash Point - See SDS

GENERAL INFORMATION

This product is not recommended for use in pure oxygen and/or oxygen rich systems and should not be selected as a sealant for chlorine or other strong oxidizing materials.

For safe handling information on this product, consult the Safety Data Sheet (SDS).

Mold Preparation
Cleaning:
Mold surfaces must be thoroughly cleaned and dried. All traces of prior release must be removed. This may be accomplished by using Frekote® PMC or other suitable cleaner. Frekote® 915WB™ or light abrasives can be used for heavy build-up.

Sealing   New/Repaired   Molds:

Occasionally, green or freshly repaired molds are rushed into service prior to complete cure causing an increased amount of free styrene on the mold surface. Fresh or "production line" repairs, new fiberglass and epoxy molds should be cured per manufacturer's instructions, usually a minimum of 2 -3 weeks at 22°C before starting full-scale production. Fully cured previously unused molds should be sealed before use. This can be accomplished by applying one to two coats of an appropriate Frekote® mold sealer, following the directions for use instructions. Allow full cure of the appropriate Frekote® mold sealer before you apply the first coat of LOCTITE® FREKOTE 770-NC™ as outlined in the directions of use.

Directions for use:

1. LOCTITE® FREKOTE 770-NC™ can be applied to mold surfaces at room temperature up to 60°C by spraying, brushing or wiping with a clean lint-free, cloth. When spraying ensure a dry air source is used or use an airless spray system. Always use in a well ventilated area.
2. Wipe or spray on a smooth, thin, continuous, wet film. Avoid wiping or spraying over the same area that was just coated until the solvent has evaporated. If spraying, hold nozzle 20 to 30cm from mold surface. It is suggested that small areas be coated, working progressively from one side of the mold to the other.
3. Initially, apply 2 to 3 base coats allowing 5 to 10 minutes between coats for solvent evaporation .
4. Allow the final coat to cure for 5 to 10 minutes at 22°C.
5. Maximum releases will be obtained as the mold surface becomes conditioned to LOCTITE® FREKOTE 770-NC™ . Performance can be enhanced by re-coating once, after the first few initial pulls.
6. When any release difficulty is experienced, the area in question can be "touched-up" by re-coating the entire mold surface or just those areas where release difficulty is occurring.
7. **NOTE**: LOCTITE® FREKOTE 770-NC™ is moisture sensitive, keep container tightly closed when not in use. The product should always be used in a well ventilated area.
8. **Precaution:** Users of closed mold systems (rotomolding) must be certain that solvent evaporation is complete and that all solvent vapors have been ventilated from the mold cavity prior to closing the mold. An oil-free compressed air source can be used to assist in evaporation of solvents and ventilation of the mold cavity.

Mold Touch up
Touch up coats should only be applied to areas where poor release is noticed and should be applied using the same

(Henkel)

method as base coats. This will reduce the possibility of release agent or polymer build-up. The frequency of touch ups will depend on the polymer type, mold configuration, and abrasion parameters.

Loctite Material Specification^{LMS}
LMS dated May 29, 2007. Test reports for each batch are available for the indicated properties. LMS test reports include selected QC test parameters considered appropriate to specifications for customer use. Additionally, comprehensive controls are in place to assure product quality and consistency. Special customer specification requirements may be coordinated through Henkel Quality.

Storage
The product is classified as flammable and must be stored in an appropriate manner in compliance with relevant regulations. Do not store near oxidizing agents or combustible materials. Store product in the unopened container in a dry location. Storage information may also be indicated on the product container labelling.
Optimal Storage: 8 °C to 21 °C. Storage below 8 °C or greater than 28 °C can adversely affect product properties. Material removed from containers may be contaminated during use. Do not return product to the original container. Henkel cannot assume responsibility for product which has been contaminated or stored under conditions other than those previously indicated. If additional information is required, please contact your local Technical Service Center or Customer Service Representive.

Conversions
(°C x 1.8) + 32 = °F
kV/mm x 25.4 = V/mil
mm / 25.4 = inches
µm / 25.4 = mil
N x 0.225 = lb
N/mm x 5.71 = lb/in
N/mm² x 145 = psi
MPa x 145 = psi
N·m x 8.851 = lb·in
N·m x 0.738 = lb·ft
N·mm x 0.142 = oz·in
mPa·s = cP

Note:
The information provided in this Technical Data Sheet (TDS) including the recommendations for use and application of the product are based on our knowledge and experience of the product as at the date of this TDS. The product can have a variety of different applications as well as differing application and working conditions in your environment that are beyond our control. Henkel is, therefore, not liable for the suitability of our product for the production processes and conditions in respect of which you use them, as well as the intended applications and results. We strongly recommend that you carry out your own prior trials to confirm such suitability of our product.
Any liability in respect of the information in the Technical Data Sheet or any other written or oral recommendation(s) regarding the concerned product is excluded, except if otherwise explicitly agreed and except in relation to death or personal injury caused by our negligence and any liability under any applicable mandatory product liability law.

In case products are delivered by Henkel Belgium NV, Henkel Electronic Materials NV, Henkel Nederland BV, Henkel Technologies France SAS and Henkel France SA please additionally note the following:
In case Henkel would be nevertheless held liable, on whatever legal ground, Henkel's liability will in no event exceed the amount of the concerned delivery.

In case products are delivered by Henkel Colombiana, S.A.S. the following disclaimer is applicable:
The information provided in this Technical Data Sheet (TDS) including the recommendations for use and application of the product are based on our

knowledge and experience of the product as at the date of this TDS. Henkel is, therefore, not liable for the suitability of our product for the production processes and conditions in respect of which you use them, as well as the intended applications and results. We strongly recommend that you carry out your own prior trials to confirm such suitability of our product.
Any liability in respect of the information in the Technical Data Sheet or any other written or oral recommendation(s) regarding the concerned product is excluded, except if otherwise explicitly agreed and except in relation to death or personal injury caused by our negligence and any liability under any applicable mandatory product liability law.

In case products are delivered by Henkel Corporation, Resin Technology Group, Inc., or Henkel Canada Corporation, the following disclaimer is applicable:
The data contained herein are furnished for information only and are believed to be reliable. We cannot assume responsibility for the results obtained by others over whose methods we have no control. It is the user's responsibility to determine suitability for the user's purpose of any production methods mentioned herein and to adopt such precautions as may be advisable for the protection of property and of persons against any hazards that may be involved in the handling and use thereof. In light of the foregoing, **Henkel Corporation specifically disclaims all warranties expressed or implied, including warranties of merchantability or fitness for a particular purpose, arising from sale or use of Henkel Corporation's products. Henkel Corporation specifically disclaims any liability for consequential or incidental damages of any kind, including lost profits.** The discussion herein of various processes or compositions is not to be interpreted as representation that they are free from domination of patents owned by others or as a license under any Henkel Corporation patents that may cover such processes or compositions. We recommend that each prospective user test his proposed application before repetitive use, using this data as a guide. This product may be covered by one or more United States or foreign patents or patent applications.

Trademark usage
Except as otherwise noted, all trademarks in this document are trademarks of Henkel Corporation in the U.S. and elsewhere. ® denotes a trademark registered in the U.S. Patent and Trademark Office.

Reference 0.1

Americas	Europe	Asia
+860.571.5100	+49.89.320800.1800	+86.21.2891.8863

For the most direct access to local sales and technical support visit www.henkel.com/industrial

---

Loctite 2014, *Loctite Frekote 770-NC Technical Data Sheet,* Henkel Adhesives, Dusseldorf, Germany, accessed 15 March 2019,
<https://tdsna.henkel.com/NA/UT/HNAUTTDS.nsf/web/5BE653876CAE92988525715C001BD4C1/$File/frekote%2055nc-en.pdf>

Appendix D: Kennametal KCN05 Bur Router

Speeds & Feeds | **Grades** | **Tolerances**

Burr-Style Router • CBDB • Inch

Material Group			Side Milling (A) and Slotting (B)	K600		beyond KCN05		Feed per Revolution — Inch per revolution (IPR) information is for Side Milling (A). For Slotting (B), reduce IPR by 10%.			
				Cutting Speed — vc SFM		Cutting Speed — vc SFM		D1 — Diameter			
			A								
			B								
			ap	min	max	min	max	frac	1/4	3/8	1/2
			ae								
			ap					IPR	.0059	.0098	.0118
C	1		Ap1 max	265	400	330	500				
			0.2 x D								
			1 x D								

NOTE: Lower value of cutting speed is used for high stock removal applications or for higher hardness (machinability) within group. Higher value of cutting speed is used for finishing applications or for lower hardness (machinability) within group. Above parameters are based on ideal conditions. For smaller taper machining centers, please adjust parameters accordingly on >1/2" diameter.

Appendix E: Tensile Test Results

SVB Hard Patch (baseline)

Specimen	Width (mm)	Thickness (mm)	Load (N)	Mpa	Comments
1	25.7	4.78	47894	389.9	
2	25.11	4.57	34116	297.3	Failure due to delamination prior to testing. Neglected from study
3	25.64	4.61	51506	435.8	
4	25.79	4.42	42372	371.7	
5	25.48	4.72	31582	262.6	Failure due to delamination prior to testing. Neglected from study
6	16.46	4.49	32158	435.1	
7	25.7	4.73	36008	296.2	Failure due to delamination prior to testing. Neglected from study
8	25.55	4.62	33938	287.5	Failure due to delamination prior to testing. Neglected from study
Average		4.62	38697	408.1	

SVB Co-cure (w/overlap)

Specimen	Width (mm)	Thickness (mm)	Load (N)	Mpa	Comments
1	25.56	4.85	36311	292.9	Failure has crack propagation extending beyond scarf.
2	25.58	4.79	44737	365.1	
3	25.44	4.63	51202	434.7	
4	25.61	4.83	51271	414.5	Failure has crack propagation extending beyond scarf.
5	25.62	4.87	46986	376.6	Failure has crack propagation extending beyond scarf.
6	25.48	4.77	35713	293.8	
7	25.64	4.79	29205	237.8	
8	25.62	4.76	33973	278.6	
9	14.35	4.58	22835	347.4	
Average		4.76	39137	337.9	

DVB Hard Patch (w/ caul plate)

Specimen	Width (mm)	Thickness (mm)	Load (N)	Mpa
1	26.57	4.18	41209	371.0
2	26	4.25	41116	372.1
3	26.2	4.30	38352	340.4
4	26.15	4.39	37780	329.1
5	26.12	4.39	48859	426.1
6	26.21	4.43	49154	423.3
7	26.24	4.38	37505	326.3
8	26.09	4.32	44276	392.8
9	25.95	4.21	42556	389.5
Average		4.32	42312	374.5

DVB Co-cure (w/overlap)

Specimen	Width (mm)	Thickness (mm)	Load (N)	Mpa
1	25.71	4.46	52899	461.3
2	25.69	4.62	45448	382.9
3	25.74	4.48	43256	375.1
4	25.61	4.85	33860	272.6
5	25.67	4.59	46170	391.9
6	25.52	4.71	46456	386.5
7	25.65	4.70	44602	370.0
8	25.76	4.72	50270	413.4
9	25.69	4.62	52268	440.4
10	25.58	4.64	49908	420.5
11	14.21	4.28	17351	285.3
Average		4.61	43863	381.8

DVB co-cure (w/offset adherend)

Specimen	Width (mm)	Thickness (mm)	Load (N)	Mpa	Comments
1	25.66	4.08	43158	412.2	Initial failure at 37kN, delamination of outer plies propagated into patch.
2	25.6	4.13	37343	353.2	Complete failure, occurred in region where visible adhesive porosity on edge was noted before test.
3	25.67	4.28	30997	282.1	Complete failure, occurred in region where visible adhesive porosity on edge was noted before test.
4	25.61	4.44	40655	357.5	Initial failure at 36kN.
5	25.67	4.35	38087	341.1	Initial failure at 34kN.
6	25.62	4.33	35119	316.6	Delamination of outer plies propagated into patch, visible porosity along bond-line
7	25.46	4.40	39593	353.4	Initial failure at 38kN with delamination along 0 degree plies, where patch was offset to account for adhesive thickness.
8	25.56	4.31	38023	345.2	Initial failure at 37kN, delamination of outer plies propagated into patch.
9	25.52	4.23	40398	374.2	Initial failure at 39kN.
10	14.22	4.18	19586	329.5	Delamination of outer plies propagated into patch, visible porosity along bond-line.
Average		4.27	36296	346.5	

DVB Co-cure (w/caul plate)

Specimen	Width (mm)	Thickness (mm)	Load (N)	Mpa
1	26.19	4.34	43695	384.4
2	25.86	4.35	45918	408.2
3	25.97	4.33	51770	460.4
4	26.36	4.41	44724	384.7
5	26.31	4.39	42708	369.8
6	26.21	4.40	47616	412.9
7	26.45	4.30	44447	390.8
Average		4.36	45840	401.6

Appendix F: Microscopy Comparison Samples

SVB Parent-to-Parent	DVB Co-Cure (w/overlap)
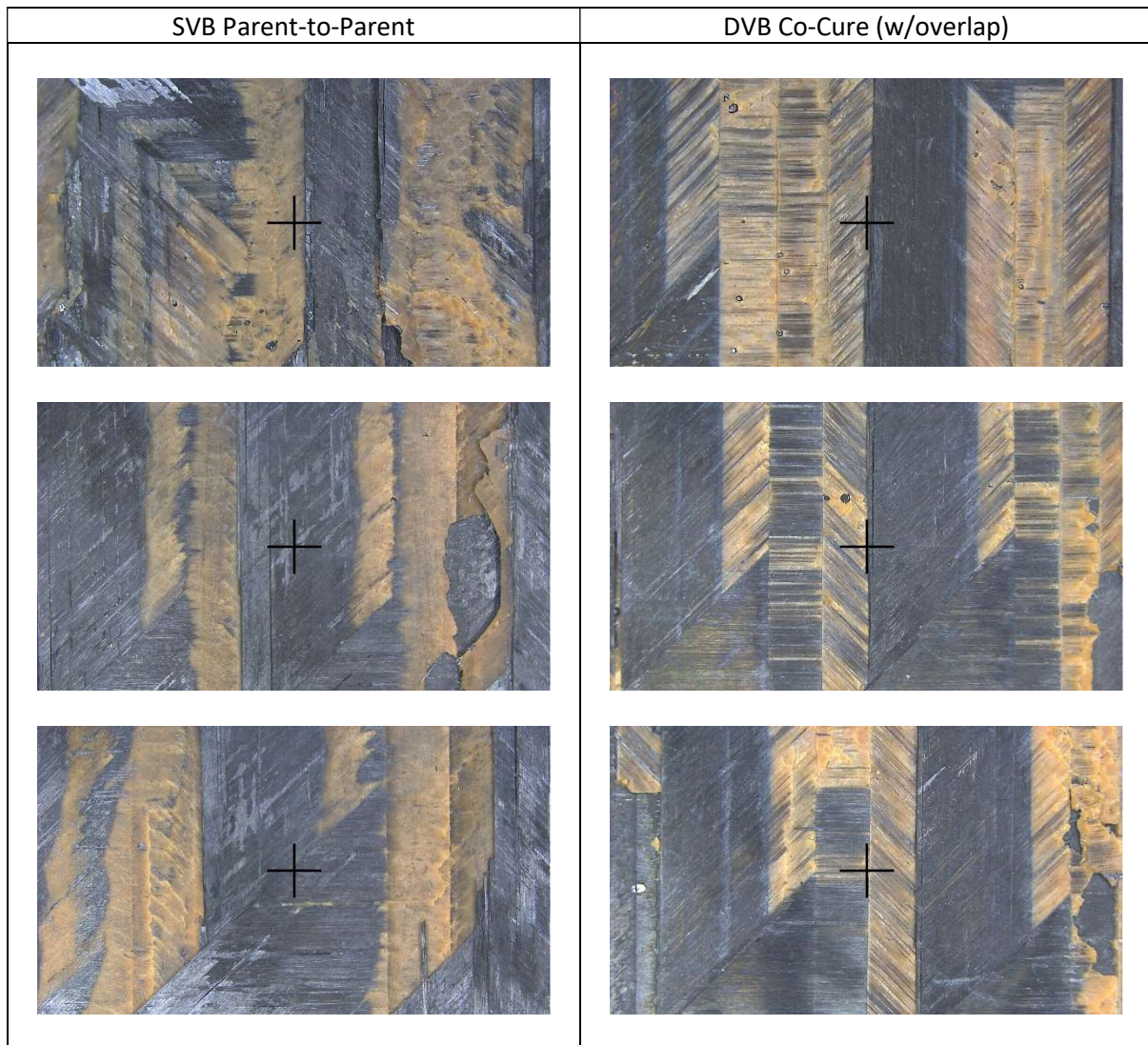
Appendix G: Failure Mechanism Images

SVB Hard Patch (baseline)
Specimen 1: 390 MPa
Specimen 5: 262 MPa
Specimen 3: 436 MPa

SVB Co-Cure (with overlap)	
Specimen 1: 292 MPa	
Specimen 4: 415 MPa	
Specimen 8: 278 MPa	

DVB Co-Cure (with overlap)	
Specimen 1: 461 MPa	
Specimen 4: 273 MPa	
Specimen 7: 370 MPa	
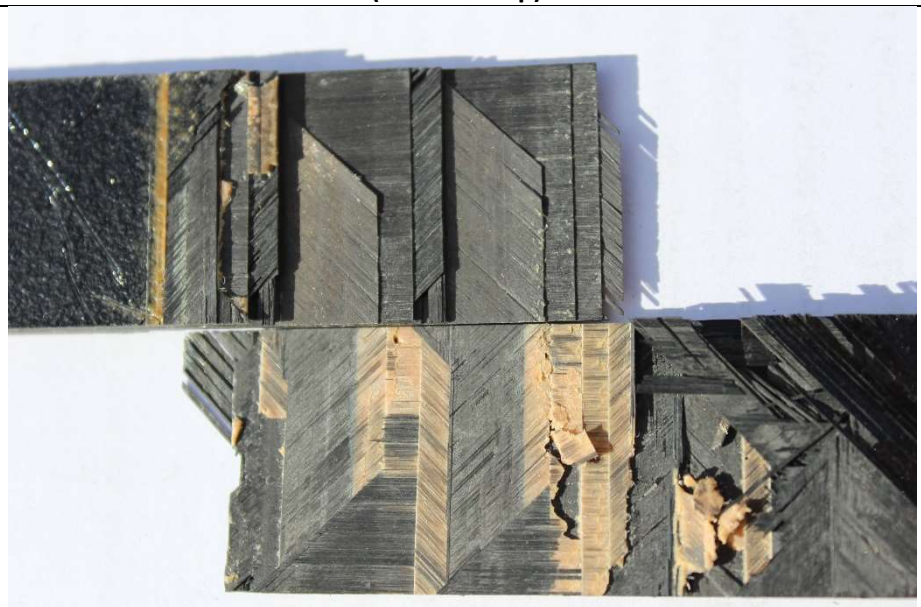
	DVB Co-Cure (with adherend offset)
Specimen 1: 412 MPa	
Specimen 2: 353 MPa	
Specimen 7: 353 MPa	

DVB Co-Cure (with caul plate)
Specimen 1: 384 MPa
Specimen 2: 408 MPa
Specimen 4: 384 MPa

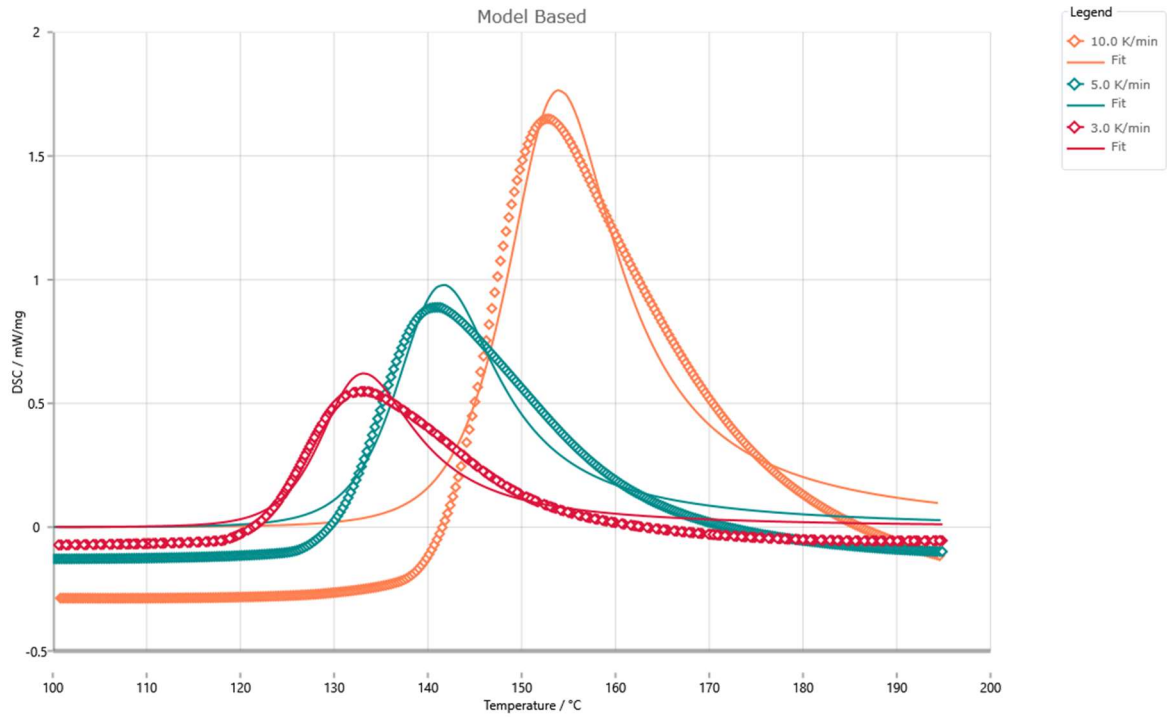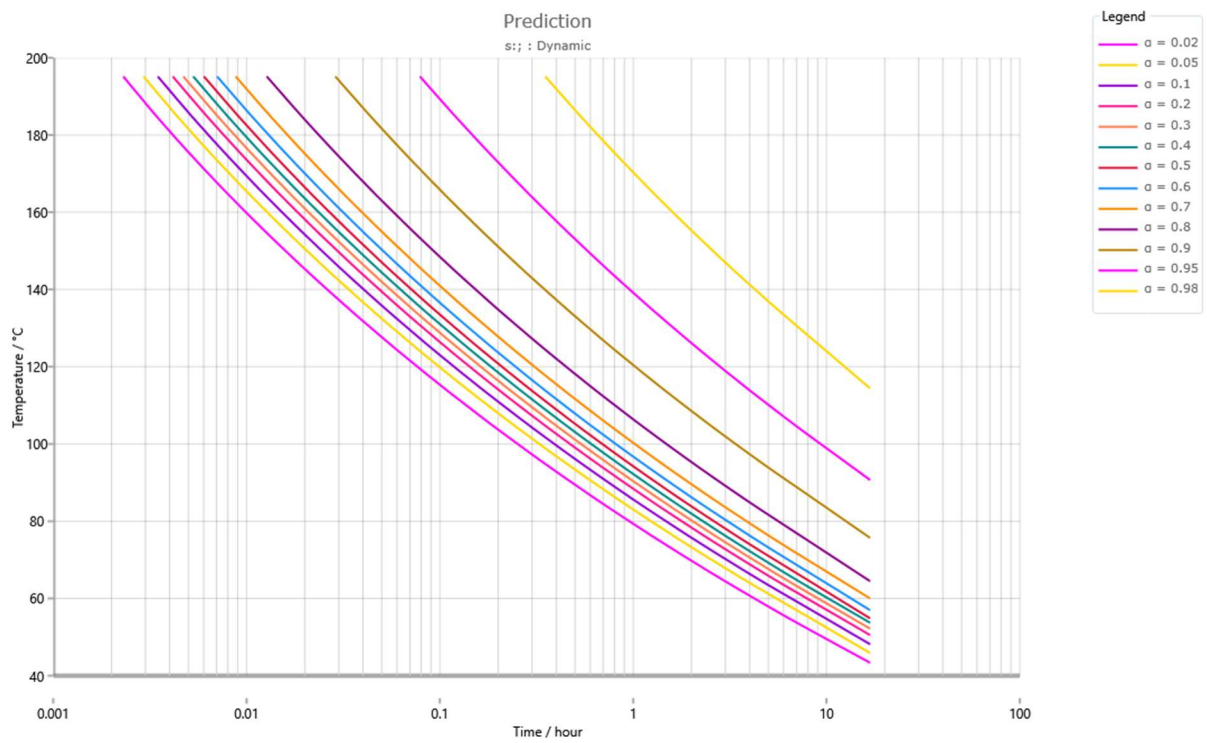| DVB Hard Patch (with caul plate)	
Specimen 1: 371 MPa	
Specimen 3: 340 MPa	
Specimen 5: 426 MPa	
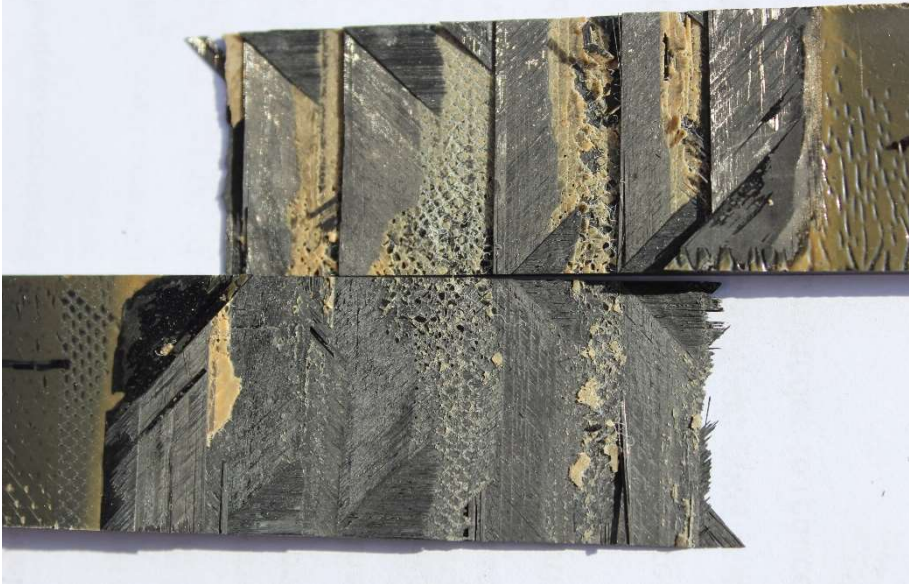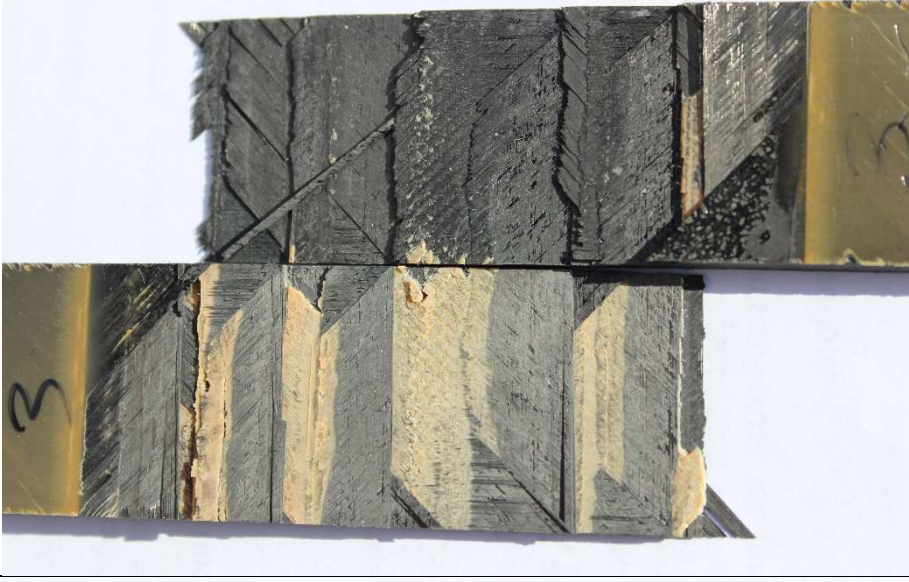
Appendix H: NETSZCH Kinetics Neo Models

Appendix H.1: Adhesive Model Fitting

Appendix H.2: Adhesive Time Temperature Transformation

Appendix G: Risk Management Plan

University of Southern Queensland

USQ Safety Risk Management System

Close

Develop as new RMP

Version 2.0

Safety Risk Management Plan

Risk Management Plan ID:	Status:	Current User:	Author:	Supervisor:	Approver: i:0#.w|usq\u8007520
RMP_2019_3799	Approval Requested	i:0#.w|usq\u1085731	i:0#.w|usq\u1085731	i:0#.w|usq\u8007520	

Assessment Title:	Prepreg layup, vacuum bag curing, heat mapping of curing and tensile testing	Assessment Date:	16/10/2019
Workplace (Division/Faculty/Section):	451000 - Centre for Future Materials	Review Date:	6/12/2019 (5 years maximum)

Approver:		Supervisor: (for notification of Risk Assessment only)	
Xuesen Zeng;		Xuesen Zeng;	

Context

DESCRIPTION:

What is the task/event/purchase/project/procedure?	layup of carbon fibre samples using prepreg (CYCOM 5320), Out of Autoclave debulking, oven cure, tensile testing
Why is it being conducted?	To characterize the mechanical properties and behaviour of the fabricated samples
Where is it being conducted?	P11, CFM
Course code (if applicable)		Chemical Name (if applicable)	Marbocote Mould Cleaner, Loctite 710-NC

WHAT ARE THE NOMINAL CONDITIONS?

Personnel involved	Riley Mitchell
Equipment	Out of Autoclave rig, curing oven for samples, MTS testing equipment
Environment	Standard lab
Other	n/a
Briefly explain the procedure/process	Layup of CF prepreg, Out of Autoclave debulking procedure, curing in the oven, bending, compaction and tensile test on required machines

Assessment Team - who is conducting the assessment?

Assessor(s):	Riley Mitchell
Others consulted: (eg elected health and safety representative, other personnel exposed to risks)	Brian Lenske

Risk Matrix

Probability	Consequence				
	Insignificant ❓ No Injury 0-$5K	Minor ❓ First Aid $5K-$50K	Moderate ❓ Med Treatment $50K-$100K	Major ❓ Serious Injury $100K-$250K	Catastrophic ❓ Death More than $250K
Almost Certain ❓ 1 in 2	M	H	E	E	E
Likely ❓ 1 in 100	M	H	H	E	E
Possible ❓ 1 in 1,000	L	M	H	H	H
Unlikely ❓ 1 in 10,000	L	L	M	M	M
Rare ❓ 1 in 1,000,000	L	L	L	L	L

Recommended Action Guide	
Extreme:	E= Extreme Risk – Task **MUST NOT** proceed
High:	H = High Risk – Special Procedures Required (Contact USQSafe) Approval by VC only
Medium:	M= Medium Risk - A Risk Management Plan/Safe Work Method Statement is required
Low:	L= Low Risk - Manage by routine procedures.

	Step 1	Step 2	Step 2a	Step 3				Step 4				
	Hazards:	**The Risk:**	**Existing Controls:**	**Risk Assessment:**				**Additional Controls:**	**Risk assessment with additional controls**			
	From step 1 or more if identified	What can happen if exposed to the hazard with existing controls in place?	What are the existing controls that are already in place?	Consequence x Probability = Risk Level				Enter additional controls if required to reduce the risk level	Has the consequence or probability changed?			
				Consequence	Probability	Risk Level	ALARP		Consequence	Probability	Risk Level	ALARP
	Example											
	Working in temperatures over 35° c	Heat stress/heat stroke/exhaustion leading to serious personal	Regular breaks, chilled water available, loose clothing, fatigue management policy.	catastrophic	possible	high	No	temporary shade shelters, essential tasks only, close supervision, buddy system	catastrophic	unlikely	mod	Yes
1	Work with carb...	Hand and eye injuries from cutting equipment.	Ensure equipment in good working order. PPE - safety glasses and gloves.	Insignifica	Possible	Low	☑					☐
2	Chemical clean...	Hand and eye injuries; respiratory discomfort.	PPE - safety glasses, gloves, lab coat and P2 respirator. SDS available.	Insignifica	Possible	Low	☑					☐
3	Vacuum bag pr...	Hand and eye injuries from cutting equipment.	Ensure equipment in good working order. PPE - safety glasses and gloves.	Insignifica	Possible	Low	☑					☐
4	Vacuum evacu...	Hand and eye injuries from vacuum line leaks.	Ensure no leaks in vacuum bag, lines and fittings. SWP's available.	Insignifica	Unlikely	Low	☑					☐
5	Curing sample ...	Burns.	PPE - heat resistant gloves and lab coat or long sleeves. Signage for warning of hot surface.	Insignifica	Possible	Low	☐	Develop SWP for Out of Autoclave equipment.	Insignifica	Possible	Low	☑
6	Using oven at 1..	Burns.	SWP available. PPE - heat resistant gloves and lab coat .	Insignifica	Possible	Low	☑					☐
7	Cutting carbon...	Respiratory discomfort, eye and skin irritation from carbon fibre dust and debris.	Use cutting room with mechanical ventilation, equipment guards and equipment SWP available. PPE - safety glasses and full face respirator, gloves, lab coat or long sleeves.	Insignifica	Possible	Low	☑					☐
8	Cutting equipm..	Thermal hazard causing burns.	Keep electrical components clean and free from carbon fibre dust build-up. PPE- lab coat or long sleeves.	Minor	Unlikely	Low	☑					☐
9	Waste disposal...	Hand and eye injuries; respiratory discomfort.	PPE - safety glasses, gloves, lab coat or long sleeves and P2 respirator. Dispose as Industrial waste.	Insignifica	Possible	Low	☑					☐
10	Sample failure ...	Hand and eye injuries.	SWP available, ensure machine guards in working order. PPE - safety glasses, gloves, lab coat or long sleeves.	Minor	Unlikely	Low	☑					☐
11	Slips/trips/falls.	Operator can injure themselves.	Ensure cables, air lines are placed away from work areas. Clean-up materials or spills immediately. Appropriate footwear with non-slip sole.	Minor	Unlikely	Low	☑					☐
12	Electrical equip..	Electric Shock.	Test and tagged leads and equipment.	Moderate	Rare	Low	☑					☐